

**Supporting Information**

**In Search of Tris(Trimethylsilylcyclopentadienyl) Thorium**

Justin C. Wedal, Samuel Bekoe, Joseph W. Ziller , Filipp Furche,\* and William J. Evans\*

Department of Chemistry, University of California, Irvine, California 92697, United States

Email: [wevans@uci.edu](mailto:wevans@uci.edu), [filipp.furche@uci.edu](mailto:filipp.furche@uci.edu)

\*To whom correspondence should be addressed

## Table of Contents

<b>Experimental Details</b>	<b>S3</b>
<b><sup>1</sup>H NMR spectra for reaction of A with MeI</b>	<b>S5</b>
<b>Crystallographic Details for:</b>	
Cp' <sub>3</sub> ThBr	S6
Figure S3: ORETP representation of Cp' <sub>3</sub> ThBr	S7
Table S1. Bond lengths [Å] and angles [°] for Cp' <sub>3</sub> ThBr	S7
Table S2. Bond lengths [Å] and angles [°] for Cp' <sub>3</sub> ThBr	S8
Cp' <sub>3</sub> ThMe	S15
Figure S4. ORETP representation of Cp' <sub>3</sub> ThMe	S17
Table S3. Bond lengths [Å] and angles [°] for Cp' <sub>3</sub> ThMe	S17
Table S4. Bond lengths [Å] and angles [°] for Cp' <sub>3</sub> ThMe	S18
(Cp' <sub>3</sub> Th) <sub>2</sub> (μ-O)	S21
Figure S5. ORETP representation of (Cp' <sub>3</sub> Th) <sub>2</sub> (μ-O)	S22
Table S5. Bond lengths [Å] and angles [°] for (Cp' <sub>3</sub> Th) <sub>2</sub> (μ-O)	S22
Table S6. Bond lengths [Å] and angles [°] for (Cp' <sub>3</sub> Th) <sub>2</sub> (μ-O)	S23
<b>Computational Details</b>	<b>S27</b>
Figure S6. Calculated dz <sup>2</sup> -like HOMO of Cp' <sub>3</sub> Th	S28
Figure S7. d-f like HOMO of (Cp' <sub>3</sub> ThBr) <sup>1-</sup> and f-like HOMO of Cp' <sub>3</sub> ThBr	S29
Figure S8. Calculated UV-visible spectra of Cp' <sub>3</sub> Th, (Cp' <sub>3</sub> ThBr) <sup>1-</sup> , and Cp' <sub>3</sub> ThBr	S29
Table S7. Electronic excitation summary of Cp' <sub>3</sub> Th, (Cp' <sub>3</sub> ThBr) <sup>1-</sup> , and Cp' <sub>3</sub> ThBr	S30
<b>Figure S9:</b> X-band EPR spectrum of (C <sub>5</sub> Me <sub>4</sub> H) <sub>3</sub> Th in toluene at 77K	S32
<b>Figure S10:</b> Decomposition of A by monitoring absorbance at 496 nm in THF	S32

## **Electrochemical Details**

<b>Figure S11:</b> Cyclic voltammogram of Cp'3ThCl with a scan rate of 200 mV/s	<b>S33</b>
<b>Figure S12:</b> Cyclic voltammogram of Cp'3ThCl with a scan rate of 500 mV/s	<b>S34</b>
<b>Figure S13:</b> Cyclic voltammogram of Cp'3ThCl with a scan rate of 1000 mV/s	<b>S34</b>
<b>References</b>	<b>S35</b>

## **Experimental Details**

**Synthesis of Cp'3ThCl from A and Me<sub>3</sub>SiCl.** Cp'3ThBr (51 mg, 0.070 mmol) in THF (1 mL) and KC<sub>8</sub> (11 mg, 0.081 mmol) were chilled in separate vials at -35 °C for two hours. The KC<sub>8</sub> was tapped into the colorless stirring solution of Cp'3ThBr to form the dark blue solution **A**. Me<sub>3</sub>SiCl (3 drops, excess) was added. No immediate color change occurred, so the solution was stirred for 40 min at which point the solution had become colorless. Black solids were removed via centrifugation and the colorless supernatant was dried under vacuum. Extraction into hexane and removal of solvent yielded white solids (36 mg). Cp'3ThCl and Cp'3ThH<sup>1</sup> were identified by <sup>1</sup>H NMR spectroscopy in an 8:1 ratio.

**Synthesis of Cp'3ThI from A and I<sub>2</sub>.** Following a similar procedure for the synthesis of Cp'3ThCl from **A**, Cp'3ThBr (48 mg, 0.066 mmol) and KC<sub>8</sub> (11 mg, 0.081 mmol) were combined to form the solution **A**. A solution of I<sub>2</sub> (18 mg, 0.071 mmol) in THF (1 mL) was added dropwise. The mixture immediately turned orange. After stirring for 5 min, the solution was dried and the solids were extracted into hexane. The solvent was removed under vacuum to yield as yellow solids (47 mg), Cp'3ThI and Cp'3ThBr were identified by <sup>1</sup>H NMR spectroscopy in a 10:1 ratio, along with a small amount of other unidentifiable peaks.

**Synthesis of Cp'3Th(C≡CPh) from A and HC≡CPh.** Following a similar procedure for the synthesis of Cp'3ThCl from **A**, Cp'3ThBr (50 mg, 0.069 mmol) and KC<sub>8</sub> (12 mg, 0.089 mmol) were combined to form solution **A**. HC≡CPh (1 drop) was added and the solution immediately became dark orange. After the solution was stirred for 5 min, volatiles were removed under vacuum to yield a dark oil. The oil was extracted into hexane to yield a green-brown solution. This solution was filtered and dried to yield brown oily solids. Cp'3Th(C≡CPh) was identified by <sup>1</sup>H NMR spectroscopy.

**Reaction of A and MeI.** Following a similar procedure for the synthesis of Cp'3ThCl from **A**, Cp'3ThBr (51 mg, 0.070 mmol) and KC<sub>8</sub> (11 mg, 0.081 mmol) were combined to form the solution **A**. MeI (1 drop) was added and the solution immediately turned colorless. After stirring for 5 min, the solution was dried and the solids were extracted into hexane. The solvent was removed under vacuum to yield white solids (44 mg). The mixture contained Cp'3ThMe and Cp'3ThI in an approximate 1 : 1.5 ratio as determined by <sup>1</sup>H NMR spectroscopy. Cp'3ThH and Cp'3ThBr were also observed in the spectrum. Other unidentifiable peaks were also present.

**Decomposition of A.** Cp'3ThBr (24 mg, 0.033 mmol) was dissolved in THF (1 mL). KC<sub>8</sub> (excess) was added and the solution immediately became the dark blue color of **A**. The solution was stirred at room temperature for 90 min at which point the solution had become colorless with black solids, presumably graphite. The solids were removed via centrifugation and the grey solution was dried under vacuum. The <sup>1</sup>H NMR spectrum in C<sub>6</sub>D<sub>6</sub> displayed multiple unidentifiable peaks, along with Cp'3ThH.<sup>1</sup> When the same reaction was done in THF-*d*<sub>8</sub>, a similar <sup>1</sup>H NMR spectrum was observed. The <sup>2</sup>H spectrum displayed only THF-*d*<sub>8</sub> peaks.

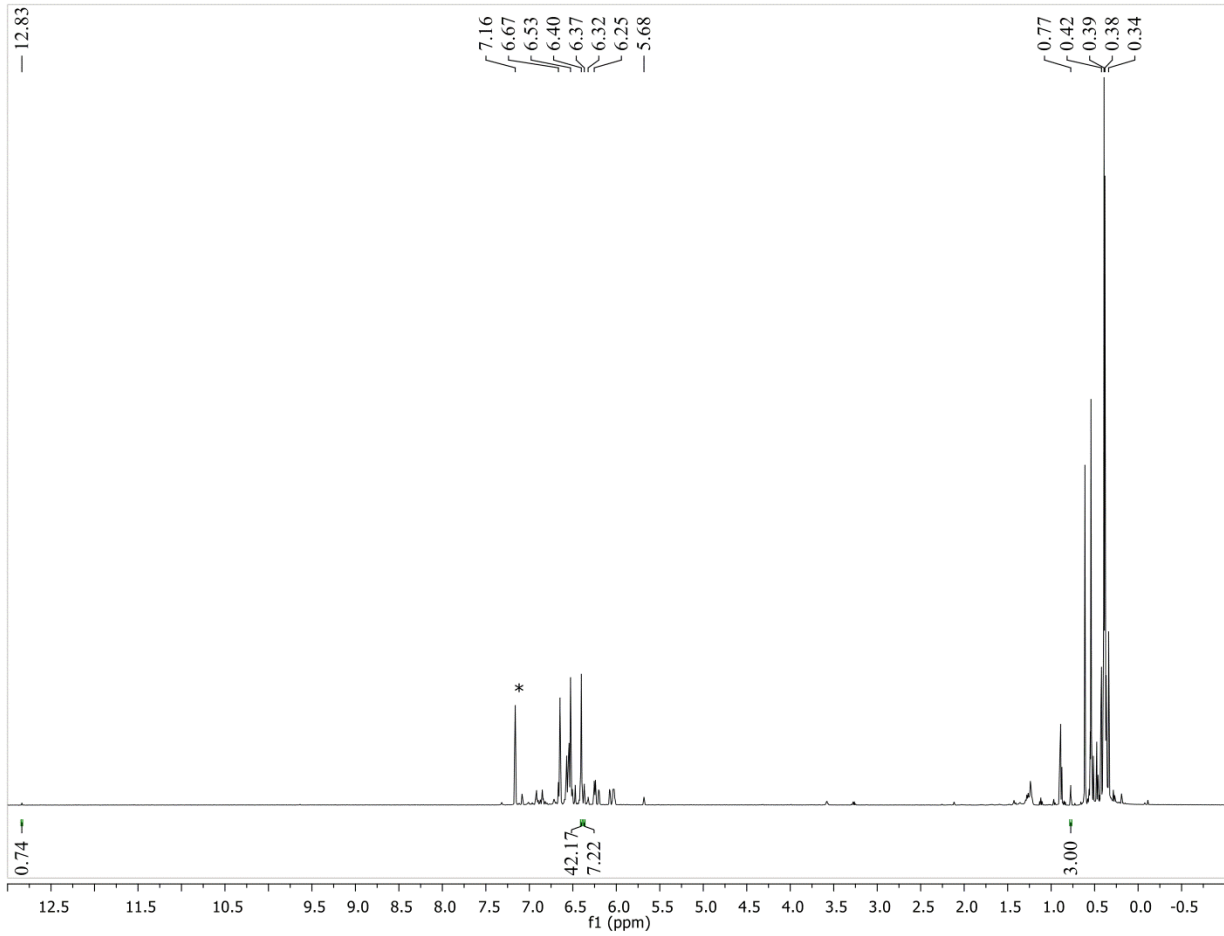


**Fig. S1.** <sup>1</sup>H NMR spectrum of reaction of **A** with MeI. Residual *C<sub>6</sub>D<sub>5</sub>H* peak is labeled with \*.

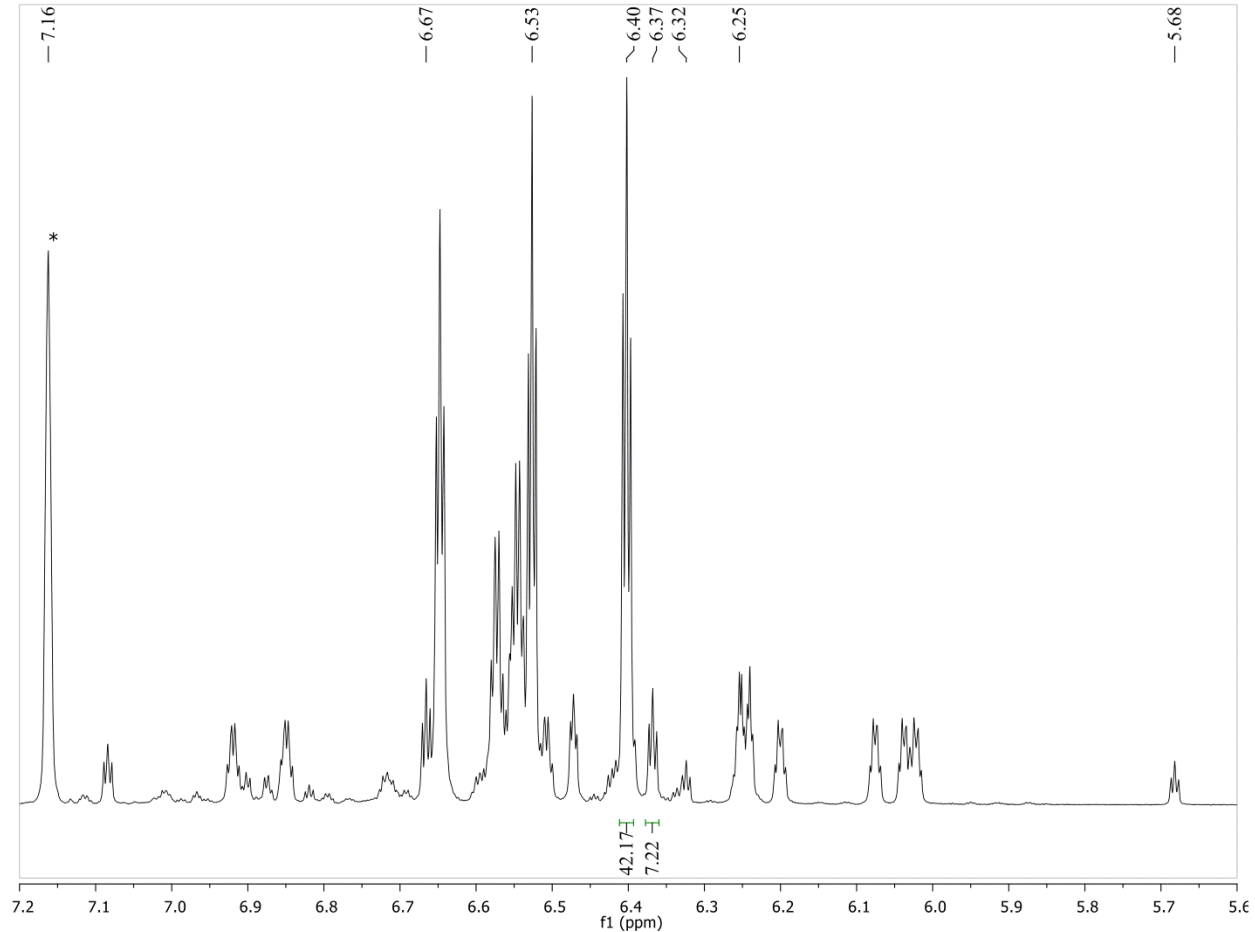


**Fig. S2.** Expanded  $^1\text{H}$  NMR spectrum of reaction of **A** with MeI. Residual  $\text{C}_6\text{D}_5\text{H}$  peak is labeled with \*.

#### X-ray Data Collection, Structure Solution and Refinement for $\text{Cp}'_3\text{ThBr}$

A colorless crystal of approximate dimensions  $0.194 \times 0.199 \times 0.258$  mm was mounted on a glass fiber and transferred to a Bruker SMART APEX II diffractometer. The APEX2<sup>2</sup> program package was used to determine the unit-cell parameters and for data collection (25 sec/frame scan time for a sphere of diffraction data). The raw frame data was processed using SAINT<sup>3</sup> and SADABS<sup>4</sup> to yield the reflection data file. Subsequent calculations were carried out

using the SHELXTL<sup>5</sup> program. The diffraction symmetry was  $2/m$  and the systematic absences were consistent with the monoclinic space group  $P2_1/c$  that was later determined to be correct. The structure was solved by direct methods and refined on  $F^2$  by full-matrix least-squares techniques. The analytical scattering factors<sup>6</sup> for neutral atoms were used throughout the analysis. Hydrogen atoms were included using a riding model. There were two molecules of the formula-unit present.

Least-squares analysis yielded  $wR2 = 0.0687$  and  $Goof = 1.073$  for 541 variables refined against 13207 data ( $0.76 \text{ \AA}$ ),  $R1 = 0.0286$  for those 10983 data with  $I > 2.0\sigma(I)$ .

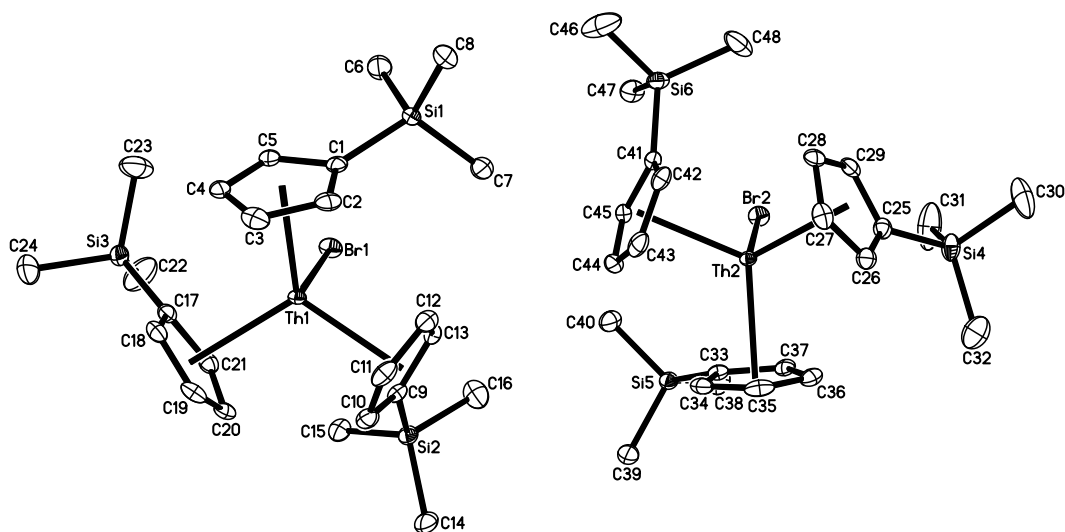


**Fig. S3.** ORETP representation of  $\text{Cp}'_3\text{ThBr}$  with thermal ellipsoids drawn at the 50% probability level. Hydrogen atoms are omitted for clarity.

**Table S1.** Crystal data and structure refinement for  $\text{Cp}'_3\text{ThBr}$ .

Identification code	jcw6 (Justin Wedal)
Empirical formula	$\text{C}_{24} \text{H}_{39} \text{BrSi}_3\text{Th}$
Formula weight	723.77
Temperature	133(2) K

Wavelength	0.71073 Å
Crystal system	Monoclinic
Space group	<i>P2<sub>1</sub>/c</i>
Unit cell dimensions	a = 21.7256(15) Å      α = 90°. b = 16.9264(12) Å      β = 91.1625(8)°. c = 15.1850(10) Å      γ = 90°.
Volume	5582.9(7) Å <sup>3</sup>
Z	8
Density (calculated)	1.722 Mg/m <sup>3</sup>
Absorption coefficient	6.911 mm <sup>-1</sup>
F(000)	2800
Crystal color	colorless
Crystal size	0.258 x 0.199 x 0.194 mm <sup>3</sup>
Theta range for data collection	1.525 to 27.894°
Index ranges	-28 ≤ <i>h</i> ≤ 28, -21 ≤ <i>k</i> ≤ 22, -19 ≤ <i>l</i> ≤ 19
Reflections collected	65691
Independent reflections	13207 [R(int) = 0.0251]
Completeness to theta = 25.500°	99.9 %
Absorption correction	Semi-empirical from equivalents
Max. and min. transmission	0.4308 and 0.2963
Refinement method	Full-matrix least-squares on F <sup>2</sup>
Data / restraints / parameters	13207 / 0 / 541
Goodness-of-fit on F <sup>2</sup>	1.073
Final R indices [I>2sigma(I) = 10983 data]	R1 = 0.0286, wR2 = 0.0656
R indices (all data, 0.76 Å)	R1 = 0.0372, wR2 = 0.0687
Largest diff. peak and hole	3.725 and -1.641 e.Å <sup>-3</sup>

**Table S2.** Bond lengths [Å] and angles [°] for Cp'<sub>3</sub>ThBr.

Th(1)-Cnt1	2.537	Th(1)-C(4)	2.792(4)
Th(1)-Cnt2	2.539	Th(1)-C(20)	2.792(4)
Th(1)-Cnt3	2.546	Th(1)-C(12)	2.798(4)
Th(1)-C(19)	2.775(4)	Th(1)-C(13)	2.803(4)
Th(1)-C(3)	2.776(4)	Th(1)-C(5)	2.811(4)
Th(1)-C(11)	2.788(4)	Th(1)-C(2)	2.819(4)

Th(1)-C(10)	2.819(4)	Th(2)-Cnt6	2.544
Th(1)-C(21)	2.826(4)	Th(2)-C(43)	2.772(4)
Th(1)-C(18)	2.826(4)	Th(2)-C(27)	2.776(4)
Th(1)-C(9)	2.834(4)	Th(2)-C(35)	2.784(4)
Th(1)-C(1)	2.840(4)	Th(2)-C(36)	2.798(4)
Th(1)-Br(1)	2.8515(4)	Th(2)-C(26)	2.803(4)
Th(1)-C(17)	2.864(4)	Th(2)-C(44)	2.808(4)
Si(1)-C(7)	1.854(4)	Th(2)-C(42)	2.817(4)
Si(1)-C(6)	1.858(4)	Th(2)-C(28)	2.822(4)
Si(1)-C(1)	1.874(4)	Th(2)-C(37)	2.823(4)
Si(1)-C(8)	1.874(5)	Th(2)-C(34)	2.827(4)
Si(2)-C(15)	1.853(4)	Th(2)-C(29)	2.828(4)
Si(2)-C(14)	1.864(4)	Th(2)-C(45)	2.831(4)
Si(2)-C(16)	1.867(5)	Th(2)-C(25)	2.839(4)
Si(2)-C(9)	1.884(4)	Th(2)-Br(2)	2.8450(4)
Si(3)-C(23)	1.853(5)	Th(2)-C(41)	2.846(4)
Si(3)-C(22)	1.859(6)	Th(2)-C(33)	2.853(4)
Si(3)-C(24)	1.861(5)	Si(4)-C(31)	1.854(6)
Si(3)-C(17)	1.868(4)	Si(4)-C(30)	1.857(5)
C(1)-C(2)	1.425(6)	Si(4)-C(32)	1.858(6)
C(1)-C(5)	1.432(5)	Si(4)-C(25)	1.869(4)
C(2)-C(3)	1.405(6)	Si(5)-C(39)	1.857(5)
C(3)-C(4)	1.414(6)	Si(5)-C(33)	1.865(4)
C(4)-C(5)	1.401(6)	Si(5)-C(40)	1.866(4)
C(9)-C(13)	1.422(5)	Si(5)-C(38)	1.875(5)
C(9)-C(10)	1.423(6)	Si(6)-C(48)	1.858(5)
C(10)-C(11)	1.406(6)	Si(6)-C(46)	1.866(5)
C(11)-C(12)	1.412(6)	Si(6)-C(41)	1.873(4)
C(12)-C(13)	1.391(6)	Si(6)-C(47)	1.874(4)
C(17)-C(21)	1.423(5)	C(25)-C(29)	1.421(6)
C(17)-C(18)	1.433(6)	C(25)-C(26)	1.422(6)
C(18)-C(19)	1.408(6)	C(26)-C(27)	1.411(6)
C(19)-C(20)	1.418(6)	C(27)-C(28)	1.413(6)
C(20)-C(21)	1.395(6)	C(28)-C(29)	1.402(6)
Th(2)-Cnt4	2.544	C(33)-C(34)	1.422(5)
Th(2)-Cnt5	2.547	C(33)-C(37)	1.434(6)

C(34)-C(35)	1.408(6)	C(19)-Th(1)-C(5)	119.42(12)
C(35)-C(36)	1.409(6)	C(3)-Th(1)-C(5)	47.99(12)
C(36)-C(37)	1.398(6)	C(11)-Th(1)-C(5)	123.74(12)
C(41)-C(45)	1.424(5)	C(4)-Th(1)-C(5)	28.96(11)
C(41)-C(42)	1.428(6)	C(20)-Th(1)-C(5)	136.55(12)
C(42)-C(43)	1.414(6)	C(12)-Th(1)-C(5)	106.61(11)
C(43)-C(44)	1.411(6)	C(13)-Th(1)-C(5)	116.80(11)
C(44)-C(45)	1.400(6)	C(19)-Th(1)-C(2)	116.46(12)
		C(3)-Th(1)-C(2)	29.07(12)
Cnt1-Th(1)-Br(1)	101.2	C(11)-Th(1)-C(2)	76.57(12)
Cnt2-Th(1)-Br(1)	101.5	C(4)-Th(1)-C(2)	47.96(12)
Cnt3-Th(1)-Br(1)	100.8	C(20)-Th(1)-C(2)	145.50(12)
Cnt1-Th(1)-Cnt2	116.2	C(12)-Th(1)-C(2)	67.51(12)
Cnt1-Th(1)-Cnt3	116.8	C(13)-Th(1)-C(2)	91.27(12)
Cnt2-Th(1)-Cnt3	116.0	C(5)-Th(1)-C(2)	47.63(12)
C(19)-Th(1)-C(3)	90.66(12)	C(19)-Th(1)-C(10)	75.31(13)
C(19)-Th(1)-C(11)	88.20(13)	C(3)-Th(1)-C(10)	113.64(13)
C(3)-Th(1)-C(11)	87.98(13)	C(11)-Th(1)-C(10)	29.03(12)
C(19)-Th(1)-C(4)	92.41(12)	C(4)-Th(1)-C(10)	142.12(12)
C(3)-Th(1)-C(4)	29.42(13)	C(20)-Th(1)-C(10)	68.04(12)
C(11)-Th(1)-C(4)	117.38(12)	C(12)-Th(1)-C(10)	47.72(12)
C(19)-Th(1)-C(20)	29.51(12)	C(13)-Th(1)-C(10)	47.54(12)
C(3)-Th(1)-C(20)	120.02(12)	C(5)-Th(1)-C(10)	152.40(12)
C(11)-Th(1)-C(20)	92.16(13)	C(2)-Th(1)-C(10)	105.60(12)
C(4)-Th(1)-C(20)	116.11(12)	C(19)-Th(1)-C(21)	47.91(12)
C(19)-Th(1)-C(12)	117.34(13)	C(3)-Th(1)-C(21)	123.90(12)
C(3)-Th(1)-C(12)	90.59(13)	C(11)-Th(1)-C(21)	119.75(12)
C(11)-Th(1)-C(12)	29.29(13)	C(4)-Th(1)-C(21)	105.24(12)
C(4)-Th(1)-C(12)	115.44(12)	C(20)-Th(1)-C(21)	28.76(12)
C(20)-Th(1)-C(12)	115.74(12)	C(12)-Th(1)-C(21)	137.89(11)
C(19)-Th(1)-C(13)	121.97(12)	C(13)-Th(1)-C(21)	116.53(11)
C(3)-Th(1)-C(13)	117.76(12)	C(5)-Th(1)-C(21)	114.40(12)
C(11)-Th(1)-C(13)	47.88(12)	C(2)-Th(1)-C(21)	152.12(12)
C(4)-Th(1)-C(13)	137.23(12)	C(10)-Th(1)-C(21)	92.89(12)
C(20)-Th(1)-C(13)	105.25(12)	C(19)-Th(1)-C(18)	29.10(12)
C(12)-Th(1)-C(13)	28.76(11)	C(3)-Th(1)-C(18)	77.66(12)

C(11)-Th(1)-C(18)	113.32(12)	C(11)-Th(1)-Br(1)	126.30(9)
C(4)-Th(1)-C(18)	68.30(12)	C(4)-Th(1)-Br(1)	103.01(9)
C(20)-Th(1)-C(18)	47.84(12)	C(20)-Th(1)-Br(1)	100.68(8)
C(12)-Th(1)-C(18)	142.03(12)	C(12)-Th(1)-Br(1)	102.44(9)
C(13)-Th(1)-C(18)	150.77(12)	C(13)-Th(1)-Br(1)	78.49(8)
C(5)-Th(1)-C(18)	92.12(12)	C(5)-Th(1)-Br(1)	78.45(8)
C(2)-Th(1)-C(18)	106.74(12)	C(2)-Th(1)-Br(1)	112.34(8)
C(10)-Th(1)-C(18)	104.37(12)	C(10)-Th(1)-Br(1)	113.37(8)
C(21)-Th(1)-C(18)	47.33(11)	C(21)-Th(1)-Br(1)	77.55(8)
C(19)-Th(1)-C(9)	95.06(12)	C(18)-Th(1)-Br(1)	113.70(8)
C(3)-Th(1)-C(9)	135.62(12)	C(9)-Th(1)-Br(1)	84.49(8)
C(11)-Th(1)-C(9)	48.42(11)	C(1)-Th(1)-Br(1)	83.58(8)
C(4)-Th(1)-C(9)	163.53(12)	C(19)-Th(1)-C(17)	48.54(12)
C(20)-Th(1)-C(9)	76.05(12)	C(3)-Th(1)-C(17)	96.91(12)
C(12)-Th(1)-C(9)	48.17(11)	C(11)-Th(1)-C(17)	136.32(12)
C(13)-Th(1)-C(9)	29.21(11)	C(4)-Th(1)-C(17)	76.28(12)
C(5)-Th(1)-C(9)	145.34(11)	C(20)-Th(1)-C(17)	48.18(11)
C(2)-Th(1)-C(9)	115.68(12)	C(12)-Th(1)-C(17)	163.81(12)
C(10)-Th(1)-C(9)	29.16(11)	C(13)-Th(1)-C(17)	145.06(11)
C(21)-Th(1)-C(9)	90.61(11)	C(5)-Th(1)-C(17)	88.97(11)
C(18)-Th(1)-C(9)	122.44(12)	C(2)-Th(1)-C(17)	123.54(12)
C(19)-Th(1)-C(1)	138.26(12)	C(10)-Th(1)-C(17)	116.13(12)
C(3)-Th(1)-C(1)	48.52(12)	C(21)-Th(1)-C(17)	28.96(11)
C(11)-Th(1)-C(1)	97.25(12)	C(18)-Th(1)-C(17)	29.16(11)
C(4)-Th(1)-C(1)	48.52(11)	C(9)-Th(1)-C(17)	119.41(11)
C(20)-Th(1)-C(1)	164.54(12)	C(1)-Th(1)-C(17)	118.30(11)
C(12)-Th(1)-C(1)	77.27(11)	Br(1)-Th(1)-C(17)	84.67(8)
C(13)-Th(1)-C(1)	90.14(11)	C(7)-Si(1)-C(6)	108.1(2)
C(5)-Th(1)-C(1)	29.36(11)	C(7)-Si(1)-C(1)	115.99(18)
C(2)-Th(1)-C(1)	29.15(11)	C(6)-Si(1)-C(1)	107.19(19)
C(10)-Th(1)-C(1)	124.11(12)	C(7)-Si(1)-C(8)	108.1(2)
C(21)-Th(1)-C(1)	142.82(11)	C(6)-Si(1)-C(8)	110.2(2)
C(18)-Th(1)-C(1)	116.81(11)	C(1)-Si(1)-C(8)	107.32(19)
C(9)-Th(1)-C(1)	119.31(11)	C(15)-Si(2)-C(14)	108.6(2)
C(19)-Th(1)-Br(1)	125.46(9)	C(15)-Si(2)-C(16)	107.5(2)
C(3)-Th(1)-Br(1)	126.24(9)	C(14)-Si(2)-C(16)	111.3(2)

C(15)-Si(2)-C(9)	115.53(18)	C(10)-C(11)-C(12)	107.5(4)
C(14)-Si(2)-C(9)	107.8(2)	C(10)-C(11)-Th(1)	76.7(2)
C(16)-Si(2)-C(9)	106.14(19)	C(12)-C(11)-Th(1)	75.7(2)
C(23)-Si(3)-C(22)	106.7(3)	C(13)-C(12)-C(11)	108.1(4)
C(23)-Si(3)-C(24)	108.3(3)	C(13)-C(12)-Th(1)	75.8(2)
C(22)-Si(3)-C(24)	109.3(3)	C(11)-C(12)-Th(1)	75.0(2)
C(23)-Si(3)-C(17)	116.1(2)	C(12)-C(13)-C(9)	109.6(4)
C(22)-Si(3)-C(17)	107.8(2)	C(12)-C(13)-Th(1)	75.4(2)
C(24)-Si(3)-C(17)	108.5(2)	C(9)-C(13)-Th(1)	76.6(2)
C(2)-C(1)-C(5)	105.4(3)	C(21)-C(17)-C(18)	105.2(4)
C(2)-C(1)-Si(1)	130.3(3)	C(21)-C(17)-Si(3)	123.4(3)
C(5)-C(1)-Si(1)	122.8(3)	C(18)-C(17)-Si(3)	129.1(3)
C(2)-C(1)-Th(1)	74.6(2)	C(21)-C(17)-Th(1)	74.0(2)
C(5)-C(1)-Th(1)	74.2(2)	C(18)-C(17)-Th(1)	74.0(2)
Si(1)-C(1)-Th(1)	126.68(17)	Si(3)-C(17)-Th(1)	130.13(18)
C(3)-C(2)-C(1)	109.3(4)	C(19)-C(18)-C(17)	109.4(4)
C(3)-C(2)-Th(1)	73.7(2)	C(19)-C(18)-Th(1)	73.4(2)
C(1)-C(2)-Th(1)	76.2(2)	C(17)-C(18)-Th(1)	76.9(2)
C(2)-C(3)-C(4)	108.0(4)	C(18)-C(19)-C(20)	107.4(4)
C(2)-C(3)-Th(1)	77.2(2)	C(18)-C(19)-Th(1)	77.5(2)
C(4)-C(3)-Th(1)	75.9(2)	C(20)-C(19)-Th(1)	75.9(2)
C(5)-C(4)-C(3)	107.7(4)	C(21)-C(20)-C(19)	107.9(4)
C(5)-C(4)-Th(1)	76.3(2)	C(21)-C(20)-Th(1)	77.0(2)
C(3)-C(4)-Th(1)	74.7(2)	C(19)-C(20)-Th(1)	74.6(2)
C(4)-C(5)-C(1)	109.5(4)	C(20)-C(21)-C(17)	110.1(4)
C(4)-C(5)-Th(1)	74.8(2)	C(20)-C(21)-Th(1)	74.3(2)
C(1)-C(5)-Th(1)	76.4(2)	C(17)-C(21)-Th(1)	77.0(2)
C(13)-C(9)-C(10)	105.6(3)	Cnt4-Th(2)-Br(2)	102.7
C(13)-C(9)-Si(2)	123.4(3)	Cnt5-Th(2)-Br(2)	100.0
C(10)-C(9)-Si(2)	129.2(3)	Cnt6-Th(2)-Br(2)	100.9
C(13)-C(9)-Th(1)	74.2(2)	Cnt4-Th(1)-Cnt5	116.1
C(10)-C(9)-Th(1)	74.9(2)	Cnt4-Th(1)-Cnt6	115.4
Si(2)-C(9)-Th(1)	127.73(18)	Cnt5-Th(1)-Cnt6	117.5
C(11)-C(10)-C(9)	109.2(4)	C(43)-Th(2)-C(27)	85.37(13)
C(11)-C(10)-Th(1)	74.3(2)	C(43)-Th(2)-C(35)	89.65(13)
C(9)-C(10)-Th(1)	76.0(2)	C(27)-Th(2)-C(35)	91.03(13)

C(43)-Th(2)-C(36)	118.89(13)	C(36)-Th(2)-C(34)	47.64(12)
C(27)-Th(2)-C(36)	92.68(12)	C(26)-Th(2)-C(34)	106.03(12)
C(35)-Th(2)-C(36)	29.24(13)	C(44)-Th(2)-C(34)	68.25(12)
C(43)-Th(2)-C(26)	110.62(13)	C(42)-Th(2)-C(34)	108.87(12)
C(27)-Th(2)-C(26)	29.30(12)	C(28)-Th(2)-C(34)	145.95(12)
C(35)-Th(2)-C(26)	76.97(13)	C(37)-Th(2)-C(34)	47.41(12)
C(36)-Th(2)-C(26)	67.84(12)	C(43)-Th(2)-C(29)	117.66(13)
C(43)-Th(2)-C(44)	29.28(13)	C(27)-Th(2)-C(29)	47.79(12)
C(27)-Th(2)-C(44)	114.64(12)	C(35)-Th(2)-C(29)	122.92(13)
C(35)-Th(2)-C(44)	90.21(13)	C(36)-Th(2)-C(29)	104.07(12)
C(36)-Th(2)-C(44)	115.68(12)	C(26)-Th(2)-C(29)	47.36(12)
C(26)-Th(2)-C(44)	138.86(12)	C(44)-Th(2)-C(29)	138.00(12)
C(43)-Th(2)-C(42)	29.31(12)	C(42)-Th(2)-C(29)	91.61(12)
C(27)-Th(2)-C(42)	74.52(12)	C(28)-Th(2)-C(29)	28.73(12)
C(35)-Th(2)-C(42)	116.51(13)	C(37)-Th(2)-C(29)	112.89(12)
C(36)-Th(2)-C(42)	144.59(12)	C(34)-Th(2)-C(29)	150.86(12)
C(26)-Th(2)-C(42)	103.80(12)	C(43)-Th(2)-C(45)	47.94(12)
C(44)-Th(2)-C(42)	47.76(12)	C(27)-Th(2)-C(45)	121.68(12)
C(43)-Th(2)-C(28)	89.87(13)	C(35)-Th(2)-C(45)	116.55(13)
C(27)-Th(2)-C(28)	29.22(12)	C(36)-Th(2)-C(45)	136.35(12)
C(35)-Th(2)-C(28)	119.97(13)	C(26)-Th(2)-C(45)	150.92(12)
C(36)-Th(2)-C(28)	115.54(12)	C(44)-Th(2)-C(45)	28.75(11)
C(26)-Th(2)-C(28)	47.79(12)	C(42)-Th(2)-C(45)	47.42(12)
C(44)-Th(2)-C(28)	114.66(12)	C(28)-Th(2)-C(45)	106.50(12)
C(42)-Th(2)-C(28)	66.98(12)	C(37)-Th(2)-C(45)	116.84(11)
C(43)-Th(2)-C(37)	126.82(12)	C(34)-Th(2)-C(45)	90.35(12)
C(27)-Th(2)-C(37)	119.38(12)	C(29)-Th(2)-C(45)	118.74(12)
C(35)-Th(2)-C(37)	47.87(12)	C(43)-Th(2)-C(25)	133.67(13)
C(36)-Th(2)-C(37)	28.79(11)	C(27)-Th(2)-C(25)	48.64(12)
C(26)-Th(2)-C(37)	91.54(12)	C(35)-Th(2)-C(25)	95.59(13)
C(44)-Th(2)-C(37)	108.53(12)	C(36)-Th(2)-C(25)	75.05(12)
C(42)-Th(2)-C(37)	155.32(12)	C(26)-Th(2)-C(25)	29.18(11)
C(28)-Th(2)-C(37)	135.38(12)	C(44)-Th(2)-C(25)	162.22(12)
C(43)-Th(2)-C(34)	79.66(13)	C(42)-Th(2)-C(25)	115.13(12)
C(27)-Th(2)-C(34)	116.97(13)	C(28)-Th(2)-C(25)	48.21(12)
C(35)-Th(2)-C(34)	29.06(13)	C(37)-Th(2)-C(25)	87.61(11)

C(34)-Th(2)-C(25)	122.05(12)	C(42)-Th(2)-C(33)	126.87(12)
C(29)-Th(2)-C(25)	29.05(11)	C(28)-Th(2)-C(33)	163.53(12)
C(45)-Th(2)-C(25)	147.51(11)	C(37)-Th(2)-C(33)	29.26(11)
C(43)-Th(2)-Br(2)	126.26(9)	C(34)-Th(2)-C(33)	28.99(11)
C(27)-Th(2)-Br(2)	127.07(9)	C(29)-Th(2)-C(33)	141.25(12)
C(35)-Th(2)-Br(2)	125.19(9)	C(45)-Th(2)-C(33)	89.94(11)
C(36)-Th(2)-Br(2)	102.74(8)	C(25)-Th(2)-C(33)	116.83(11)
C(26)-Th(2)-Br(2)	115.94(8)	Br(2)-Th(2)-C(33)	81.92(8)
C(44)-Th(2)-Br(2)	103.48(9)	C(41)-Th(2)-C(33)	118.96(11)
C(42)-Th(2)-Br(2)	111.36(8)	C(31)-Si(4)-C(30)	109.2(3)
C(28)-Th(2)-Br(2)	101.95(9)	C(31)-Si(4)-C(32)	110.0(3)
C(37)-Th(2)-Br(2)	77.70(8)	C(30)-Si(4)-C(32)	107.1(3)
C(34)-Th(2)-Br(2)	110.41(8)	C(31)-Si(4)-C(25)	111.5(2)
C(29)-Th(2)-Br(2)	79.30(9)	C(30)-Si(4)-C(25)	106.6(2)
C(45)-Th(2)-Br(2)	78.65(8)	C(32)-Si(4)-C(25)	112.3(2)
C(25)-Th(2)-Br(2)	86.87(8)	C(39)-Si(5)-C(33)	107.9(2)
C(43)-Th(2)-C(41)	48.72(12)	C(39)-Si(5)-C(40)	107.2(2)
C(27)-Th(2)-C(41)	96.09(12)	C(33)-Si(5)-C(40)	115.33(19)
C(35)-Th(2)-C(41)	136.64(13)	C(39)-Si(5)-C(38)	110.1(2)
C(36)-Th(2)-C(41)	163.81(12)	C(33)-Si(5)-C(38)	108.2(2)
C(26)-Th(2)-C(41)	123.80(12)	C(40)-Si(5)-C(38)	108.0(2)
C(44)-Th(2)-C(41)	48.18(11)	C(48)-Si(6)-C(46)	109.1(3)
C(42)-Th(2)-C(41)	29.21(11)	C(48)-Si(6)-C(41)	115.3(2)
C(28)-Th(2)-C(41)	77.50(12)	C(46)-Si(6)-C(41)	107.0(2)
C(37)-Th(2)-C(41)	144.46(11)	C(48)-Si(6)-C(47)	107.5(2)
C(34)-Th(2)-C(41)	116.18(12)	C(46)-Si(6)-C(47)	109.4(3)
C(29)-Th(2)-C(41)	91.87(12)	C(41)-Si(6)-C(47)	108.41(19)
C(45)-Th(2)-C(41)	29.06(11)	C(29)-C(25)-C(26)	105.4(4)
C(25)-Th(2)-C(41)	120.79(11)	C(29)-C(25)-Si(4)	122.9(3)
Br(2)-Th(2)-C(41)	82.71(8)	C(26)-C(25)-Si(4)	128.5(3)
C(43)-Th(2)-C(33)	100.79(13)	C(29)-C(25)-Th(2)	75.1(2)
C(27)-Th(2)-C(33)	138.42(12)	C(26)-C(25)-Th(2)	74.0(2)
C(35)-Th(2)-C(33)	48.41(12)	Si(4)-C(25)-Th(2)	131.70(18)
C(36)-Th(2)-C(33)	48.21(12)	C(27)-C(26)-C(25)	109.5(4)
C(26)-Th(2)-C(33)	116.05(12)	C(27)-C(26)-Th(2)	74.3(2)
C(44)-Th(2)-C(33)	79.37(12)	C(25)-C(26)-Th(2)	76.8(2)

C(26)-C(27)-C(28)	107.6(4)	C(35)-C(36)-Th(2)	74.8(2)
C(26)-C(27)-Th(2)	76.4(2)	C(36)-C(37)-C(33)	109.2(4)
C(28)-C(27)-Th(2)	77.2(2)	C(36)-C(37)-Th(2)	74.6(2)
C(29)-C(28)-C(27)	107.5(4)	C(33)-C(37)-Th(2)	76.5(2)
C(29)-C(28)-Th(2)	75.9(2)	C(45)-C(41)-C(42)	105.5(3)
C(27)-C(28)-Th(2)	73.6(2)	C(45)-C(41)-Si(6)	122.8(3)
C(28)-C(29)-C(25)	109.9(4)	C(42)-C(41)-Si(6)	129.9(3)
C(28)-C(29)-Th(2)	75.4(2)	C(45)-C(41)-Th(2)	74.9(2)
C(25)-C(29)-Th(2)	75.9(2)	C(42)-C(41)-Th(2)	74.3(2)
C(34)-C(33)-C(37)	105.4(4)	Si(6)-C(41)-Th(2)	127.53(18)
C(34)-C(33)-Si(5)	127.6(3)	C(43)-C(42)-C(41)	109.2(4)
C(37)-C(33)-Si(5)	125.1(3)	C(43)-C(42)-Th(2)	73.6(2)
C(34)-C(33)-Th(2)	74.5(2)	C(41)-C(42)-Th(2)	76.5(2)
C(37)-C(33)-Th(2)	74.2(2)	C(44)-C(43)-C(42)	107.4(4)
Si(5)-C(33)-Th(2)	128.49(18)	C(44)-C(43)-Th(2)	76.8(2)
C(35)-C(34)-C(33)	109.6(4)	C(42)-C(43)-Th(2)	77.1(2)
C(35)-C(34)-Th(2)	73.8(2)	C(45)-C(44)-C(43)	108.2(4)
C(33)-C(34)-Th(2)	76.5(2)	C(45)-C(44)-Th(2)	76.5(2)
C(34)-C(35)-C(36)	107.5(4)	C(43)-C(44)-Th(2)	73.9(2)
C(34)-C(35)-Th(2)	77.2(2)	C(44)-C(45)-C(41)	109.6(4)
C(36)-C(35)-Th(2)	75.9(2)	C(44)-C(45)-Th(2)	74.7(2)
C(37)-C(36)-C(35)	108.3(4)	C(41)-C(45)-Th(2)	76.1(2)
C(37)-C(36)-Th(2)	76.6(2)		

### X-ray Data Collection, Structure Solution and Refinement for Cp'3ThMe

A colorless crystal of approximate dimensions 0.143 x 0.145 x 0.247 mm was mounted in a cryoloop and transferred to a Bruker SMART APEX II diffractometer. The APEX2<sup>2</sup> program package was used to determine the unit-cell parameters and for data collection (20 sec/frame scan time for a sphere of diffraction data). The raw frame data was processed using SAINT<sup>3</sup> and SADABS<sup>4</sup> to yield the reflection data file. The systematic absences were consistent with the

trigonal space groups  $P3$  and  $P\bar{3}$ . The centrosymmetric space group  $P\bar{3}$  was assigned and later determined to be correct.

The structure was solved by dual space methods and refined on  $F^2$  by full-matrix least-squares techniques.<sup>5</sup> The analytical scattering factors<sup>6</sup> for neutral atoms were used throughout the analysis. Hydrogen atoms were included using a riding model. The molecule was located on a three-fold rotation axis.

Least-squares analysis yielded  $wR2 = 0.0303$  and  $Goof = 1.046$  for 91 variables refined against 2483 data ( $0.73 \text{ \AA}$ ),  $R1 = 0.0143$  for those 2357 data with  $I > 2.0\sigma(I)$ .

There were several high residuals present in the final difference-Fourier map. It was not possible to determine the nature of the residuals although it was probable that diethyl ether solvent was present. The SQUEEZE<sup>7a</sup> routine in the PLATON<sup>7b</sup> program package was used to account for the electrons in the solvent accessible voids.

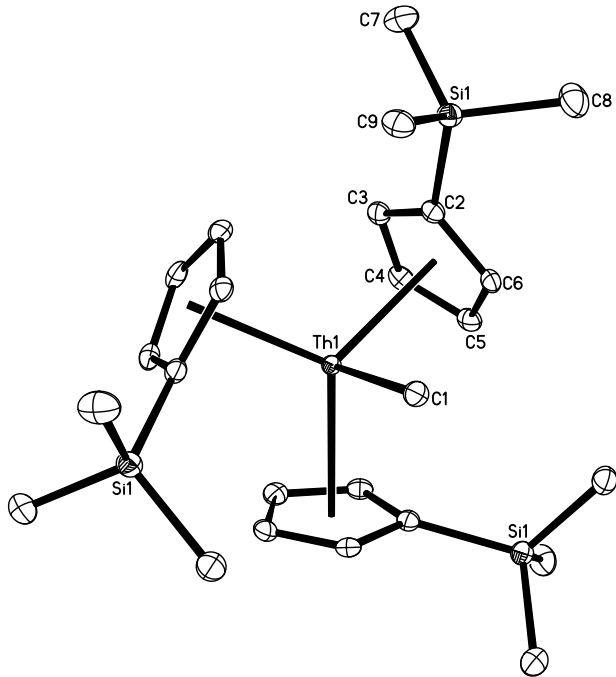


**Fig. S4.** OTREP representation of  $\text{Cp}'_3\text{ThMe}$  with thermal ellipsoids drawn at the 50% probability level. Hydrogen atoms are omitted for clarity.

**Table S3.** Crystal data and structure refinement for  $\text{Cp}'_3\text{ThMe}$ .

Identification code	jcw4 (Justin Wedal)		
Empirical formula	$\text{C}_{25} \text{H}_{42} \text{Si}_3 \text{Th}$		
Formula weight	658.89		
Temperature	88(2) K		
Wavelength	0.71073 Å		
Crystal system	Trigonal		
Space group	$P\bar{3}$		
Unit cell dimensions	$a = 15.740(2)$ Å	$\alpha = 90^\circ$ .	
	$b = 15.740(2)$ Å	$\beta = 90^\circ$ .	
	$c = 6.7581(9)$ Å	$\gamma = 120^\circ$ .	
Volume	$1450.0(4)$ Å <sup>3</sup>		
Z	2		
Density (calculated)	1.509 Mg/m <sup>3</sup>		

Absorption coefficient	5.275 mm <sup>-1</sup>
F(000)	648
Crystal color	colorless
Crystal size	0.247 x 0.145 x 0.143 mm <sup>3</sup>
Theta range for data collection	1.494 to 29.104°
Index ranges	-21 ≤ <i>h</i> ≤ 20, -20 ≤ <i>k</i> ≤ 20, -8 ≤ <i>l</i> ≤ 9
Reflections collected	17774
Independent reflections	2483 [R(int) = 0.0292]
Completeness to theta = 25.500°	100.0 %
Absorption correction	Semi-empirical from equivalents
Max. and min. transmission	0.4318 and 0.3061
Refinement method	Full-matrix least-squares on F <sup>2</sup>
Data / restraints / parameters	2483 / 0 / 91
Goodness-of-fit on F <sup>2</sup>	1.046
Final R indices [I>2sigma(I) = 2357 data]	R1 = 0.0143, wR2 = 0.0298
R indices (all data, 0.73 Å)	R1 = 0.0162, wR2 = 0.0303
Largest diff. peak and hole	0.664 and -0.424 e.Å <sup>-3</sup>

**Table S4.** Bond lengths [Å] and angles [°] for Cp'<sub>3</sub>ThMe.

Th(1)-Cnt	2.559	Th(1)-C(2)#1	2.8714(17)
Th(1)-C(1)	2.518(3)	Si(1)-C(7)	1.8667(19)
Th(1)-C(4)	2.7923(16)	Si(1)-C(8)	1.868(2)
Th(1)-C(4)#1	2.7923(17)	Si(1)-C(9)	1.8798(19)
Th(1)-C(4)#2	2.7923(17)	Si(1)-C(2)	1.8825(17)
Th(1)-C(5)	2.8081(17)	C(2)-C(3)	1.425(2)
Th(1)-C(5)#1	2.8081(17)	C(2)-C(6)	1.429(2)
Th(1)-C(5)#2	2.8081(17)	C(3)-C(4)	1.408(2)
Th(1)-C(3)#2	2.8307(17)	C(4)-C(5)	1.414(2)
Th(1)-C(3)#1	2.8307(17)	C(5)-C(6)	1.407(2)
Th(1)-C(3)	2.8307(17)		
Th(1)-C(6)	2.8409(16)	Cnt-Th(1)-C(1)	97.7
Th(1)-C(6)#1	2.8409(16)	Cnt-Th(1)-Cnt	118.2
Th(1)-C(6)#2	2.8409(16)	C(1)-Th(1)-C(4)	121.64(4)
Th(1)-C(2)	2.8713(17)	C(1)-Th(1)-C(4)#1	121.64(4)

C(4)-Th(1)-C(4)#1	95.00(5)	C(4)#1-Th(1)-C(3)	77.99(5)
C(1)-Th(1)-C(4)#2	121.64(4)	C(4)#2-Th(1)-C(3)	119.47(5)
C(4)-Th(1)-C(4)#2	95.00(5)	C(5)-Th(1)-C(3)	47.71(5)
C(4)#1-Th(1)-C(4)#2	95.00(5)	C(5)#1-Th(1)-C(3)	72.01(5)
C(1)-Th(1)-C(5)	96.51(4)	C(5)#2-Th(1)-C(3)	148.65(5)
C(4)-Th(1)-C(5)	29.24(5)	C(3)#2-Th(1)-C(3)	106.77(4)
C(4)#1-Th(1)-C(5)	123.30(5)	C(3)#1-Th(1)-C(3)	106.77(4)
C(4)#2-Th(1)-C(5)	98.35(5)	C(1)-Th(1)-C(6)	74.01(3)
C(1)-Th(1)-C(5)#1	96.51(4)	C(4)-Th(1)-C(6)	47.68(5)
C(4)-Th(1)-C(5)#1	98.35(5)	C(4)#1-Th(1)-C(6)	121.74(5)
C(4)#1-Th(1)-C(5)#1	29.24(5)	C(4)#2-Th(1)-C(6)	125.50(5)
C(4)#2-Th(1)-C(5)#1	123.30(5)	C(5)-Th(1)-C(6)	28.83(5)
C(5)-Th(1)-C(5)#1	118.733(15)	C(5)#1-Th(1)-C(6)	103.09(5)
C(1)-Th(1)-C(5)#2	96.51(4)	C(5)#2-Th(1)-C(6)	138.02(5)
C(4)-Th(1)-C(5)#2	123.29(5)	C(3)#2-Th(1)-C(6)	97.19(5)
C(4)#1-Th(1)-C(5)#2	98.35(5)	C(3)#1-Th(1)-C(6)	149.76(5)
C(4)#2-Th(1)-C(5)#2	29.24(5)	C(3)-Th(1)-C(6)	47.24(5)
C(5)-Th(1)-C(5)#2	118.732(15)	C(1)-Th(1)-C(6)#1	74.01(3)
C(5)#1-Th(1)-C(5)#2	118.732(14)	C(4)-Th(1)-C(6)#1	125.50(5)
C(1)-Th(1)-C(3)#2	112.05(4)	C(4)#1-Th(1)-C(6)#1	47.68(5)
C(4)-Th(1)-C(3)#2	77.99(5)	C(4)#2-Th(1)-C(6)#1	121.74(5)
C(4)#1-Th(1)-C(3)#2	119.47(5)	C(5)-Th(1)-C(6)#1	138.02(5)
C(4)#2-Th(1)-C(3)#2	28.99(5)	C(5)#1-Th(1)-C(6)#1	28.83(5)
C(5)-Th(1)-C(3)#2	72.01(5)	C(5)#2-Th(1)-C(6)#1	103.09(5)
C(5)#1-Th(1)-C(3)#2	148.65(5)	C(3)#2-Th(1)-C(6)#1	149.76(5)
C(5)#2-Th(1)-C(3)#2	47.71(5)	C(3)#1-Th(1)-C(6)#1	47.24(5)
C(1)-Th(1)-C(3)#1	112.05(4)	C(3)-Th(1)-C(6)#1	97.19(5)
C(4)-Th(1)-C(3)#1	119.47(5)	C(6)-Th(1)-C(6)#1	112.72(3)
C(4)#1-Th(1)-C(3)#1	28.99(5)	C(1)-Th(1)-C(6)#2	74.01(3)
C(4)#2-Th(1)-C(3)#1	77.99(5)	C(4)-Th(1)-C(6)#2	121.74(5)
C(5)-Th(1)-C(3)#1	148.65(5)	C(4)#1-Th(1)-C(6)#2	125.50(5)
C(5)#1-Th(1)-C(3)#1	47.71(5)	C(4)#2-Th(1)-C(6)#2	47.68(5)
C(5)#2-Th(1)-C(3)#1	72.01(5)	C(5)-Th(1)-C(6)#2	103.09(5)
C(3)#2-Th(1)-C(3)#1	106.77(4)	C(5)#1-Th(1)-C(6)#2	138.02(5)
C(1)-Th(1)-C(3)	112.05(3)	C(5)#2-Th(1)-C(6)#2	28.83(5)
C(4)-Th(1)-C(3)	29.00(5)	C(3)#2-Th(1)-C(6)#2	47.24(5)

C(3)#1-Th(1)-C(6)#2	97.19(5)	C(6)#1-Th(1)-C(2)#1	28.97(5)
C(3)-Th(1)-C(6)#2	149.76(5)	C(6)#2-Th(1)-C(2)#1	89.92(5)
C(6)-Th(1)-C(6)#2	112.72(3)	C(2)-Th(1)-C(2)#1	118.584(14)
C(6)#1-Th(1)-C(6)#2	112.72(3)	C(7)-Si(1)-C(8)	110.61(10)
C(1)-Th(1)-C(2)	83.12(3)	C(7)-Si(1)-C(9)	108.85(9)
C(4)-Th(1)-C(2)	48.18(5)	C(8)-Si(1)-C(9)	107.00(9)
C(4)#1-Th(1)-C(2)	93.34(5)	C(7)-Si(1)-C(2)	107.27(8)
C(4)#2-Th(1)-C(2)	142.86(5)	C(8)-Si(1)-C(2)	106.69(8)
C(5)-Th(1)-C(2)	48.11(5)	C(9)-Si(1)-C(2)	116.40(8)
C(5)#1-Th(1)-C(2)	74.72(5)	C(3)-C(2)-C(6)	105.53(14)
C(5)#2-Th(1)-C(2)	166.40(5)	C(3)-C(2)-Si(1)	126.23(13)
C(3)#2-Th(1)-C(2)	119.88(5)	C(6)-C(2)-Si(1)	125.83(13)
C(3)#1-Th(1)-C(2)	120.79(5)	C(3)-C(2)-Th(1)	73.95(9)
C(3)-Th(1)-C(2)	28.94(5)	C(6)-C(2)-Th(1)	74.33(9)
C(6)-Th(1)-C(2)	28.97(5)	Si(1)-C(2)-Th(1)	130.42(7)
C(6)#1-Th(1)-C(2)	89.92(5)	C(4)-C(3)-C(2)	109.44(15)
C(6)#2-Th(1)-C(2)	141.01(5)	C(4)-C(3)-Th(1)	73.99(9)
C(1)-Th(1)-C(2)#1	83.12(3)	C(2)-C(3)-Th(1)	77.11(9)
C(4)-Th(1)-C(2)#1	142.86(5)	C(3)-C(4)-C(5)	107.84(15)
C(4)#1-Th(1)-C(2)#1	48.18(5)	C(3)-C(4)-Th(1)	77.02(9)
C(4)#2-Th(1)-C(2)#1	93.34(5)	C(5)-C(4)-Th(1)	76.00(9)
C(5)-Th(1)-C(2)#1	166.40(5)	C(6)-C(5)-C(4)	107.69(15)
C(5)#1-Th(1)-C(2)#1	48.11(5)	C(6)-C(5)-Th(1)	76.88(9)
C(5)#2-Th(1)-C(2)#1	74.72(5)	C(4)-C(5)-Th(1)	74.76(9)
C(3)#2-Th(1)-C(2)#1	120.79(5)	C(5)-C(6)-C(2)	109.49(15)
C(3)#1-Th(1)-C(2)#1	28.94(5)	C(5)-C(6)-Th(1)	74.29(9)
C(3)-Th(1)-C(2)#1	119.88(5)	C(2)-C(6)-Th(1)	76.70(9)
C(6)-Th(1)-C(2)#1	141.01(5)		

---

Symmetry transformations used to generate equivalent atoms:

#1 -y+1,x-y,z #2 -x+y+1,-x+1,z

### X-ray Data Collection, Structure Solution and Refinement for $(\text{Cp}'_3\text{Th})_2(\mu-\text{O})$

A colorless crystal of approximate dimensions 0.112 x 0.205 x 0.329 mm was mounted in a cryoloop and transferred to a Bruker SMART APEX II diffractometer. The APEX2<sup>2</sup> program package was used to determine the unit-cell parameters and for data collection (15 sec/frame scan time for a sphere of diffraction data). The raw frame data was processed using SAINT<sup>3</sup> and SADABS<sup>4</sup> to yield the reflection data file. Subsequent calculations were carried out using the SHELXTL<sup>5</sup> program. The diffraction symmetry was  $2/m$  and the systematic absences were consistent with the monoclinic space group  $P2_1/c$  that was later determined to be correct.

The structure was solved by dual space methods and refined on  $F^2$  by full-matrix least-squares techniques. The analytical scattering factors<sup>6</sup> for neutral atoms were used throughout the analysis. Hydrogen atoms were located from a difference-Fourier map and refined ( $x,y,z$  and  $U_{\text{iso}}$ ). The molecule was located on an inversion center.

Least-squares analysis yielded  $wR2 = 0.0331$  and  $\text{Goof} = 1.037$  for 415 variables refined against 6849 data (0.73 Å),  $R1 = 0.0162$  for those 6208 data with  $I > 2.0\sigma(I)$ .

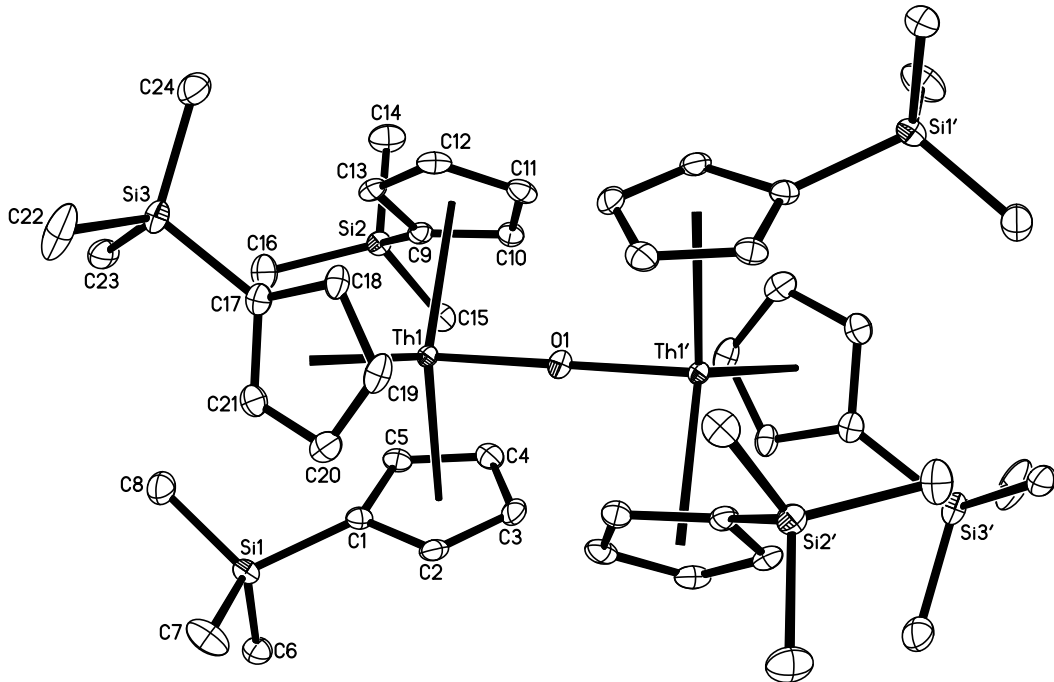


**Fig. S5.** OTREP representation of  $(\text{Cp}'_3\text{Th})_2(\mu\text{-O})$  with thermal ellipsoids drawn at the 50% probability level. Hydrogen atoms are omitted for clarity.

**Table S5.** Crystal data and structure refinement for  $(\text{Cp}'_3\text{Th})_2(\mu\text{-O})$ .

Identification code	jcw5 (Justin Wedal)		
Empirical formula	$\text{C}_{48} \text{H}_{78} \text{O Si}_6 \text{Th}_2$		
Formula weight	1303.72		
Temperature	88(2) K		
Wavelength	0.71073 Å		
Crystal system	Monoclinic		
Space group	$P2_1/c$		
Unit cell dimensions	$a = 9.5444(6)$ Å	$\alpha = 90^\circ$ .	
	$b = 18.4598(11)$ Å	$\beta = 103.9575(7)^\circ$ .	
	$c = 15.7099(10)$ Å	$\gamma = 90^\circ$ .	
Volume	$2686.2(3)$ Å <sup>3</sup>		
Z	2		

Density (calculated)	1.612 Mg/m <sup>3</sup>
Absorption coefficient	5.695 mm <sup>-1</sup>
F(000)	1276
Crystal color	colorless
Crystal size	0.329 x 0.205 x 0.112 mm <sup>3</sup>
Theta range for data collection	1.732 to 29.155°
Index ranges	-13 ≤ <i>h</i> ≤ 12, -24 ≤ <i>k</i> ≤ 23, -20 ≤ <i>l</i> ≤ 20
Reflections collected	32844
Independent reflections	6849 [R(int) = 0.0256]
Completeness to theta = 25.500°	100.0 %
Absorption correction	Semi-empirical from equivalents
Max. and min. transmission	0.4319 and 0.3096
Refinement method	Full-matrix least-squares on F <sup>2</sup>
Data / restraints / parameters	6849 / 0 / 415
Goodness-of-fit on F <sup>2</sup>	1.037
Final R indices [I>2sigma(I) = 6208 data]	R1 = 0.0162, wR2 = 0.0320
R indices (all data, 0.73 Å)	R1 = 0.0201, wR2 = 0.0331
Largest diff. peak and hole	0.565 and -0.498 e.Å <sup>-3</sup>

**Table S6.** Bond lengths [Å] and angles [°] for (Cp'<sub>3</sub>Th)<sub>2</sub>(μ-O).

Th(1)-Cnt1	2.594	Th(1)-C(2)	2.8865(19)
Th(1)-Cnt2	2.595	Th(1)-C(17)	2.9034(19)
Th(1)-Cnt3	2.587	Th(1)-C(9)	2.9217(19)
Th(1)-O(1)	2.14604(12)	Th(1)-C(1)	2.9229(18)
Th(1)-C(4)	2.803(2)	Si(1)-C(7)	1.863(2)
Th(1)-C(20)	2.8053(19)	Si(1)-C(6)	1.866(2)
Th(1)-C(12)	2.809(2)	Si(1)-C(1)	1.867(2)
Th(1)-C(21)	2.8386(19)	Si(1)-C(8)	1.867(2)
Th(1)-C(19)	2.8401(19)	Si(2)-C(9)	1.861(2)
Th(1)-C(11)	2.841(2)	Si(2)-C(14)	1.864(2)
Th(1)-C(3)	2.842(2)	Si(2)-C(16)	1.866(2)
Th(1)-C(5)	2.8419(19)	Si(2)-C(15)	1.872(2)
Th(1)-C(13)	2.8453(19)	Si(3)-C(24)	1.861(2)
Th(1)-C(18)	2.8752(19)	Si(3)-C(23)	1.863(2)
Th(1)-C(10)	2.884(2)	Si(3)-C(22)	1.867(3)

Si(3)-C(17)	1.869(2)	C(20)-Th(1)-C(19)	28.81(6)
O(1)-Th(1)#1	2.14611(12)	C(12)-Th(1)-C(19)	97.62(6)
C(1)-C(5)	1.422(3)	C(21)-Th(1)-C(19)	47.13(6)
C(1)-C(2)	1.428(3)	O(1)-Th(1)-C(11)	73.80(4)
C(2)-C(3)	1.403(3)	C(4)-Th(1)-C(11)	98.59(6)
C(3)-C(4)	1.406(3)	C(20)-Th(1)-C(11)	139.89(6)
C(4)-C(5)	1.415(3)	C(12)-Th(1)-C(11)	28.83(6)
C(9)-C(13)	1.424(3)	C(21)-Th(1)-C(11)	133.89(6)
C(9)-C(10)	1.429(3)	C(19)-Th(1)-C(11)	111.97(6)
C(10)-C(11)	1.401(3)	O(1)-Th(1)-C(3)	75.23(4)
C(11)-C(12)	1.407(3)	C(4)-Th(1)-C(3)	28.83(6)
C(12)-C(13)	1.410(3)	C(20)-Th(1)-C(3)	97.73(6)
C(17)-C(21)	1.423(3)	C(12)-Th(1)-C(3)	141.47(6)
C(17)-C(18)	1.425(3)	C(21)-Th(1)-C(3)	112.25(6)
C(18)-C(19)	1.403(3)	C(19)-Th(1)-C(3)	113.11(6)
C(19)-C(20)	1.405(3)	C(11)-Th(1)-C(3)	113.86(6)
C(20)-C(21)	1.409(3)	O(1)-Th(1)-C(5)	120.67(4)
		C(4)-Th(1)-C(5)	29.02(6)
Cnt1-Th(1)-O(1)	100.1	C(20)-Th(1)-C(5)	106.21(6)
Cnt2-Th(1)-O(1)	98.6	C(12)-Th(1)-C(5)	121.90(6)
Cnt3-Th(1)-O(1)	98.8	C(21)-Th(1)-C(5)	97.37(6)
Cnt1-Th(1)-Cnt2	117.4	C(19)-Th(1)-C(5)	134.71(6)
Cnt1-Th(1)-Cnt3	117.5	C(11)-Th(1)-C(5)	113.30(6)
Cnt2-Th(1)-Cnt3	117.6	C(3)-Th(1)-C(5)	47.12(6)
O(1)-Th(1)-C(4)	93.17(4)	O(1)-Th(1)-C(13)	119.58(4)
O(1)-Th(1)-C(20)	92.25(4)	C(4)-Th(1)-C(13)	105.04(6)
C(4)-Th(1)-C(20)	119.96(6)	C(20)-Th(1)-C(13)	123.05(6)
O(1)-Th(1)-C(12)	92.62(4)	C(12)-Th(1)-C(13)	28.86(6)
C(4)-Th(1)-C(12)	119.88(6)	C(21)-Th(1)-C(13)	98.05(6)
C(20)-Th(1)-C(12)	119.50(6)	C(19)-Th(1)-C(13)	113.28(6)
O(1)-Th(1)-C(21)	119.51(4)	C(11)-Th(1)-C(13)	47.05(6)
C(4)-Th(1)-C(21)	122.32(6)	C(3)-Th(1)-C(13)	133.58(6)
C(20)-Th(1)-C(21)	28.91(6)	C(5)-Th(1)-C(13)	96.44(6)
C(12)-Th(1)-C(21)	105.60(6)	O(1)-Th(1)-C(18)	88.77(4)
O(1)-Th(1)-C(19)	73.92(4)	C(4)-Th(1)-C(18)	167.12(6)
C(4)-Th(1)-C(19)	141.11(6)	C(20)-Th(1)-C(18)	47.19(6)

C(12)-Th(1)-C(18)	72.69(6)	C(11)-Th(1)-C(17)	105.23(6)
C(21)-Th(1)-C(18)	46.81(6)	C(3)-Th(1)-C(17)	140.90(6)
C(19)-Th(1)-C(18)	28.40(6)	C(5)-Th(1)-C(17)	116.83(6)
C(11)-Th(1)-C(18)	94.18(6)	C(13)-Th(1)-C(17)	75.37(6)
C(3)-Th(1)-C(18)	141.38(6)	C(18)-Th(1)-C(17)	28.55(5)
C(5)-Th(1)-C(18)	143.62(6)	C(10)-Th(1)-C(17)	120.80(6)
C(13)-Th(1)-C(18)	84.92(6)	C(2)-Th(1)-C(17)	112.64(6)
O(1)-Th(1)-C(10)	88.15(4)	O(1)-Th(1)-C(9)	116.39(4)
C(4)-Th(1)-C(10)	73.38(6)	C(4)-Th(1)-C(9)	77.01(6)
C(20)-Th(1)-C(10)	166.58(6)	C(20)-Th(1)-C(9)	146.88(6)
C(12)-Th(1)-C(10)	47.09(6)	C(12)-Th(1)-C(9)	47.62(6)
C(21)-Th(1)-C(10)	144.43(6)	C(21)-Th(1)-C(9)	118.27(6)
C(19)-Th(1)-C(10)	140.24(6)	C(19)-Th(1)-C(9)	141.72(6)
C(11)-Th(1)-C(10)	28.32(6)	C(11)-Th(1)-C(9)	47.22(5)
C(3)-Th(1)-C(10)	95.35(6)	C(3)-Th(1)-C(9)	105.15(6)
C(5)-Th(1)-C(10)	84.98(6)	C(5)-Th(1)-C(9)	74.42(6)
C(13)-Th(1)-C(10)	46.62(6)	C(13)-Th(1)-C(9)	28.55(5)
C(18)-Th(1)-C(10)	119.43(6)	C(18)-Th(1)-C(9)	113.44(6)
O(1)-Th(1)-C(2)	90.26(4)	C(10)-Th(1)-C(9)	28.48(5)
C(4)-Th(1)-C(2)	47.14(6)	C(2)-Th(1)-C(9)	120.04(6)
C(20)-Th(1)-C(2)	73.11(6)	C(17)-Th(1)-C(9)	101.47(5)
C(12)-Th(1)-C(2)	166.89(6)	O(1)-Th(1)-C(1)	118.39(4)
C(21)-Th(1)-C(2)	83.96(6)	C(4)-Th(1)-C(1)	47.71(6)
C(19)-Th(1)-C(2)	95.46(6)	C(20)-Th(1)-C(1)	78.02(6)
C(11)-Th(1)-C(2)	142.08(6)	C(12)-Th(1)-C(1)	144.83(6)
C(3)-Th(1)-C(2)	28.34(6)	C(21)-Th(1)-C(1)	74.63(6)
C(5)-Th(1)-C(2)	46.61(6)	C(19)-Th(1)-C(1)	106.25(6)
C(13)-Th(1)-C(2)	142.60(6)	C(11)-Th(1)-C(1)	141.79(6)
C(18)-Th(1)-C(2)	120.18(6)	C(3)-Th(1)-C(1)	47.23(6)
C(10)-Th(1)-C(2)	120.31(6)	C(5)-Th(1)-C(1)	28.51(5)
O(1)-Th(1)-C(17)	116.99(4)	C(13)-Th(1)-C(1)	116.11(6)
C(4)-Th(1)-C(17)	145.58(6)	C(18)-Th(1)-C(1)	120.70(5)
C(20)-Th(1)-C(17)	47.71(6)	C(10)-Th(1)-C(1)	113.48(5)
C(12)-Th(1)-C(17)	77.28(6)	C(2)-Th(1)-C(1)	28.46(5)
C(21)-Th(1)-C(17)	28.68(6)	C(17)-Th(1)-C(1)	100.30(5)
C(19)-Th(1)-C(17)	47.29(6)	C(9)-Th(1)-C(1)	100.29(5)

C(7)-Si(1)-C(6)	108.11(12)	C(1)-C(5)-Th(1)	78.91(11)
C(7)-Si(1)-C(1)	110.96(11)	C(13)-C(9)-C(10)	105.31(17)
C(6)-Si(1)-C(1)	107.35(10)	C(13)-C(9)-Si(2)	123.93(15)
C(7)-Si(1)-C(8)	111.51(13)	C(10)-C(9)-Si(2)	127.21(15)
C(6)-Si(1)-C(8)	107.16(11)	C(13)-C(9)-Th(1)	72.75(11)
C(1)-Si(1)-C(8)	111.52(10)	C(10)-C(9)-Th(1)	74.31(11)
C(9)-Si(2)-C(14)	106.84(10)	Si(2)-C(9)-Th(1)	134.29(9)
C(9)-Si(2)-C(16)	110.40(10)	C(11)-C(10)-C(9)	109.37(18)
C(14)-Si(2)-C(16)	106.99(12)	C(11)-C(10)-Th(1)	74.13(11)
C(9)-Si(2)-C(15)	112.55(10)	C(9)-C(10)-Th(1)	77.22(11)
C(14)-Si(2)-C(15)	108.42(11)	C(10)-C(11)-C(12)	108.26(18)
C(16)-Si(2)-C(15)	111.36(11)	C(10)-C(11)-Th(1)	77.55(11)
C(24)-Si(3)-C(23)	111.69(11)	C(12)-C(11)-Th(1)	74.33(11)
C(24)-Si(3)-C(22)	108.81(14)	C(11)-C(12)-C(13)	107.39(18)
C(23)-Si(3)-C(22)	107.38(13)	C(11)-C(12)-Th(1)	76.84(12)
C(24)-Si(3)-C(17)	112.43(10)	C(13)-C(12)-Th(1)	76.98(11)
C(23)-Si(3)-C(17)	110.92(10)	C(12)-C(13)-C(9)	109.65(18)
C(22)-Si(3)-C(17)	105.26(11)	C(12)-C(13)-Th(1)	74.16(11)
Th(1)-O(1)-Th(1)#1	180.0	C(9)-C(13)-Th(1)	78.70(11)
C(5)-C(1)-C(2)	105.39(17)	C(21)-C(17)-C(18)	105.66(18)
C(5)-C(1)-Si(1)	124.30(15)	C(21)-C(17)-Si(3)	123.43(15)
C(2)-C(1)-Si(1)	127.08(15)	C(18)-C(17)-Si(3)	127.02(15)
C(5)-C(1)-Th(1)	72.58(10)	C(21)-C(17)-Th(1)	73.13(11)
C(2)-C(1)-Th(1)	74.36(11)	C(18)-C(17)-Th(1)	74.63(11)
Si(1)-C(1)-Th(1)	133.66(9)	Si(3)-C(17)-Th(1)	134.58(9)
C(3)-C(2)-C(1)	109.39(18)	C(19)-C(18)-C(17)	109.17(18)
C(3)-C(2)-Th(1)	74.05(11)	C(19)-C(18)-Th(1)	74.41(11)
C(1)-C(2)-Th(1)	77.19(11)	C(17)-C(18)-Th(1)	76.82(11)
C(2)-C(3)-C(4)	108.28(18)	C(18)-C(19)-C(20)	108.25(18)
C(2)-C(3)-Th(1)	77.61(11)	C(18)-C(19)-Th(1)	77.19(11)
C(4)-C(3)-Th(1)	74.05(11)	C(20)-C(19)-Th(1)	74.22(11)
C(3)-C(4)-C(5)	107.31(18)	C(19)-C(20)-C(21)	107.58(18)
C(3)-C(4)-Th(1)	77.12(11)	C(19)-C(20)-Th(1)	76.97(11)
C(5)-C(4)-Th(1)	77.02(11)	C(21)-C(20)-Th(1)	76.86(11)
C(4)-C(5)-C(1)	109.62(18)	C(20)-C(21)-C(17)	109.32(18)
C(4)-C(5)-Th(1)	73.96(11)	C(20)-C(21)-Th(1)	74.24(11)

C(17)-C(21)-Th(1) 78.19(11)

---

Symmetry transformations used to generate equivalent atoms:

#1 -x+1,-y+1,-z+1

## Computational Details

Density functional theory (DFT) using the TPSSh<sup>8</sup> functional with Grimme's D3 dispersion correction<sup>9</sup> was employed to study Cp'₃ThBr, (Cp'₃ThBr)<sup>1-</sup> and Cp'₃Th species. Scalar relativistic effective core potentials (ECPs)<sup>10</sup> with the def-TZVP<sup>11</sup> basis set was used for the thorium and polarized split-valence basis sets with diffuse functions def2-SVPD<sup>12</sup> was used for the other atoms. A grid size of m4 was used. Solvent effects were accounted for using the continuum solvent model (COSMO)<sup>13</sup> with a dielectric constant of THF ( $\epsilon = 7.52$ ). All structures were computed in the C1 symmetry with geometry convergence of  $10^{-5}$  a.u and energy convergence of  $10^{-7}$  a.u. Vibrational frequencies were computed for all the optimized structures and were confirmed to be ground state structures with the absence of imaginary frequencies. Free energies and equilibrium constants at 298.15 K were obtained within the rigid rotor-harmonic oscillator approximation. All calculations were carried out with the TURBOMOLE v.7.2.1 molecular package.<sup>14</sup>

The solvent optimized structure of Cp'₃Th shows a 6dz<sup>2</sup>-like HOMO orbital in Figure S4 consistent with previous calculations on Cp''₃Th.<sup>15</sup> For comparison, Cp'₃Th was also optimized with def2-SV(P) basis set<sup>12</sup> for the lighter atoms. The average Th-Cp ring centroid distance was shortened by 0.04 Å for Cp'₃Th. The HOMO of (Cp'₃ThBr)<sup>1-</sup> shows 55% 4f-contribution and 45% 6d-contribution while the HOMO of Cp'₃ThBr shows little to no 6d-contribution, Figure S5.

Time dependent density functional theory (TDDFT) calculations were carried out on the solvent-optimized structures of Cp'₃ThBr, (Cp'₃ThBr)<sup>1-</sup>, and Cp'₃Th using the same functional

and basis sets. TDDFT calculations of the 30 lowest excitations from the spin unrestricted excitations were computed to simulate their UV-Vis spectra, Figure S6. To account for the systematic underestimation of excitation energies by semi-local density functionals such as TPSSh<sup>16</sup>, the simulated excitation spectrum was blue-shifted by 0.4 eV. Normalized Gaussian line profiles with a root mean square width of 0.12 eV were centered at the thus obtained excitation energies, scaled by the computed oscillator strength, and superimposed to simulate the experimental absorption spectra. Some notable excitations (in nm) and oscillator strengths in the length gauge (in a.u.) from each band, and dominant single-particle contributions for each transition, are reported in Table S7.

Electronic transitions were analyzed with VMD<sup>17</sup> and Mulliken population analysis (MPA). Excitations between 400 and 1000 nm are largely metal-metal transitions with d-f character for the Cp'3Th complex. Transitions below 400 nm are mostly d-p and some f-f transitions. Excitations in (Cp'3ThBr)<sup>1-</sup> are mostly f-f between 400 and 1000 nm and f-d below 350 nm. Excitations in Cp'3ThBr are largely f-f transitions below 400 nm.

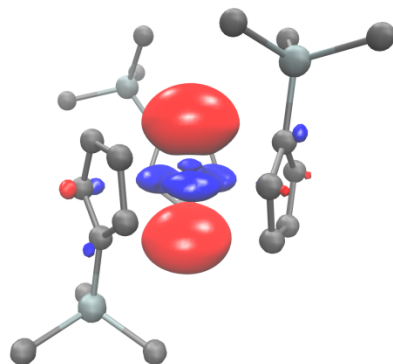


**Fig. S6.** Calculated  $dz^2$ -like HOMO of Cp'3Th plotted with a contour value of 0.06.

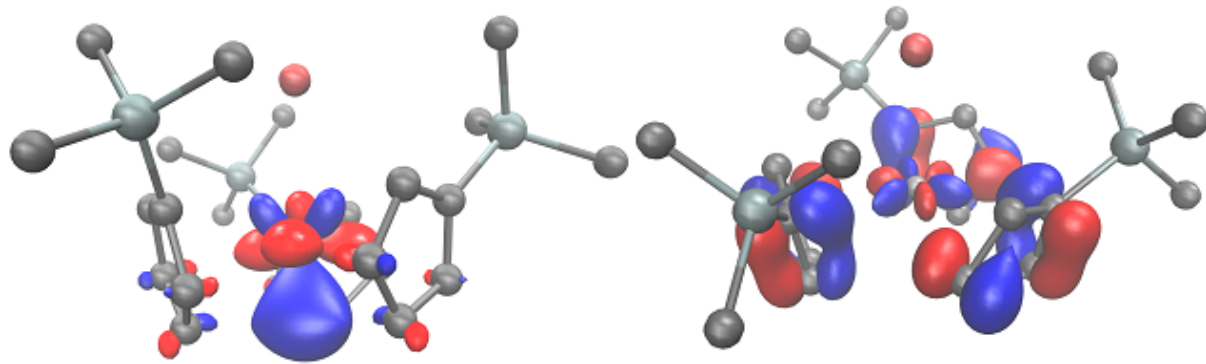


**Fig. S7.** Calculated d-f like HOMO of  $(\text{Cp}'_3\text{ThBr})^{1-}$  (left) and f-like HOMO of  $\text{Cp}'_3\text{ThBr}$  (right) plotted with contour values of 0.06.

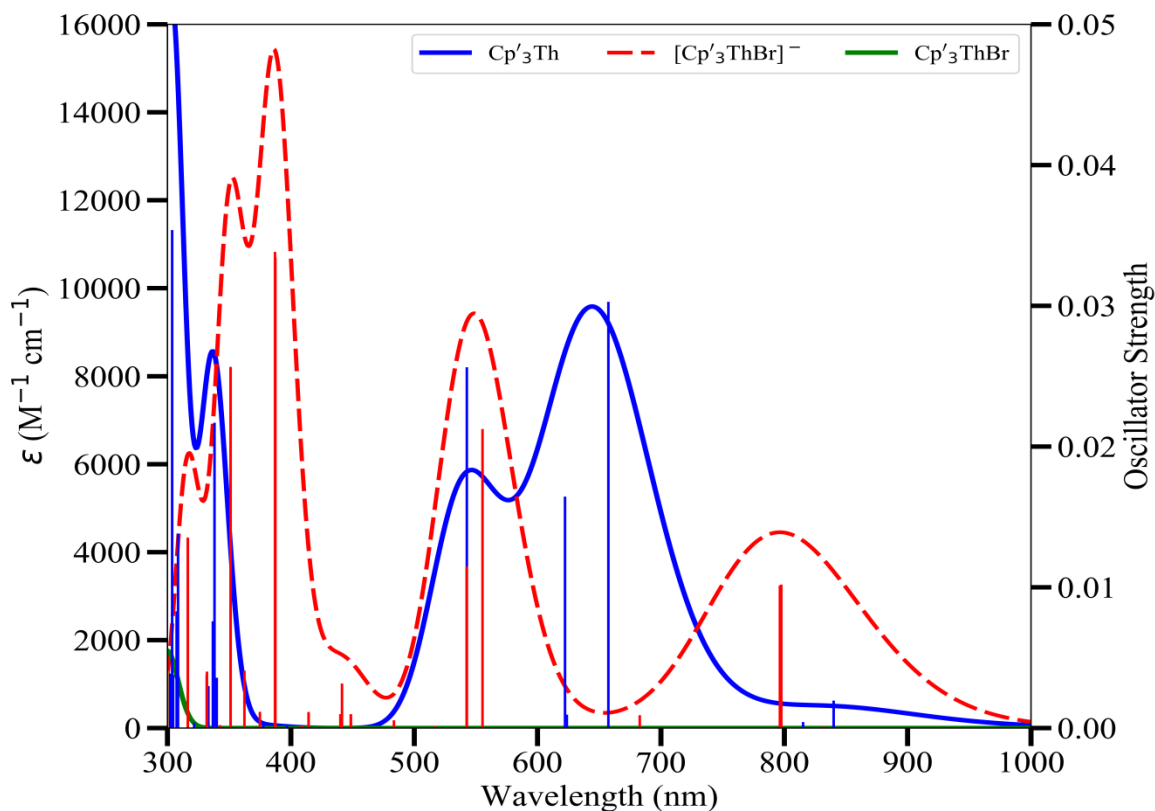


**Fig. S8.** Calculated UV-visible spectra of  $\text{Cp}'_3\text{Th}$  (solid blue),  $(\text{Cp}'_3\text{ThBr})^{1-}$  (dotted red), and  $\text{Cp}'_3\text{ThBr}$  (solid green) with computed TDDFT oscillator strengths shown as vertical lines. The

computed excitation energies were empirically blue-shifted by 0.04 eV and a gaussian line broadening of 0.12 eV were applied.

**Table S7.** Electronic excitation summary of Cp'3Th, (Cp'3ThBr)<sup>1-</sup> and Cp'3ThBr computed using TPSSh functional, def-TZVP/ECPs basis set for thorium and def2-SVPPD basis set for lighter atoms. Oscillator strength is reported in the length gauge. The 128a and 146a orbitals are the singly occupied HOMO for Cp'3Th and (Cp'3ThBr)<sup>1-</sup>, respectively, and 145a is the doubly occupied HOMO for Cp'3ThBr.

	Wavelength (nm)	Oscillator Strength (len)	Dominant Contributions			
			occupied	virtual	% weight	Transition
<b>Cp'3Th</b>	1152	0.002	128a	129a	98.8	6d-5f
	1106	0.001	128a	130a	99.1	6d-5f
	834.1	0.031	128a	131a	95.2	6d-5f
	778.4	0.016	128a	133a	96.5	6d-5f
	657.9	0.026	128a	134a	96.1	6d-5f
	381.7	0.003	128a	140a	65.1	6d-5f
			128a	137a	10.7	6d-7p
	379.6	0.022	128a	138a	55	6d-7p
			128a	139a	18.9	6d-7p
			128a	141a	11.6	6d-6d
	336.8	0.035	126b	128b	67.6	4f-7s
			128a	143a	7.8	6d-5f/6d-6d
<b>(Cp'3ThBr)<sup>1-</sup></b>	317.2	0.002	126a	130a	34.7	4f-5f
			126b	130b	31.3	4f-5f
	303.6	0.002	127a	131a	39.4	4f-5f
			127b	131b	8.3	4f-5f
	1073.8	0.01	146a	151a	89.1	4f-5f
	1071.6	0.01	146a	152a	88.9	4f-5f
	676.6	0.02	146a	153a	91.1	4f-5f
	657.8	0.011	146a	154a	90.3	4f-5f
	478.3	0.011	146a	160a	69.8	4f-5f

		146a	165a	17.9	4f-5f	
442.7	0.033	146a	167a	66.8	4f-5f	
442.4	0.034	146a	168a	67	4f-5f	
396	0.026	146a	171a	70.5	4f-5f	
352.3	0.013	146a	178a	39.9	4f-5f	
		146a	182a	19.2	4f-5f	
		146a	177a	12.1	4f-5f	
		146a	180a	10.5	4f-6d	
<b>Cp'3ThBr</b>	<b>332</b>	<b>0.004</b>	<b>145a</b>	<b>147a</b>	<b>94.7</b>	<b>4f-5f</b>
332	0.004	145a	148a	94.7	4f-5f	
296	0.008	144a	148a	40.8	4f-5f	
		143a	147a	39.2	4f-5f	
295.1	0.025	143a	147a	30.6	4f-5f	
		144a	148a	29.8	4f-5f	
		144a	147a	12.9	4f-5f	
		143a	148a	12.5	4f-5f	
295	0.022	143a	148a	30.8	4f-5f	
		144a	147a	29.5	4f-5f	
		143a	147a	12.8	4f-5f	
		144a	148a	12.6	4f-5f	
291.6	0.016	142a	146a	90.9	6p-5f	
284.7	0.02	145a	150a	53.1	4f-5f	
		142a	148a	25.1	6p-5f	
249.2	0.076	144a	151a	25.4	4f-5f	
		143a	150a	25.4	4f-5f	
		140a	148a	16.1	5d-5f	
		141a	147a	15.9	5d-5f	

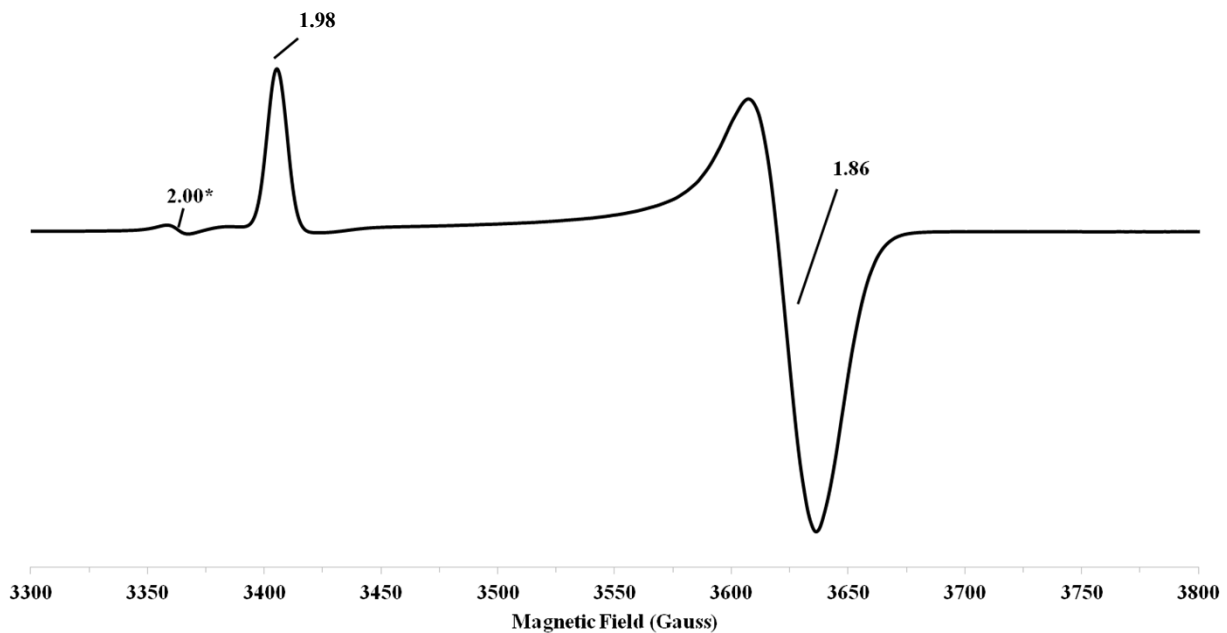


**Fig. S9.** X-band EPR spectrum of  $(\text{C}_5\text{Me}_4\text{H})_3\text{Th}^{18}$  in toluene at 77K (mode: perpendicular,  $\nu = 9.434531$  GHz,  $P = 2.161$ , modulation amplitude = 2 mT). \*The feature at  $g = 2.00$  is attributed to electride.<sup>19</sup>

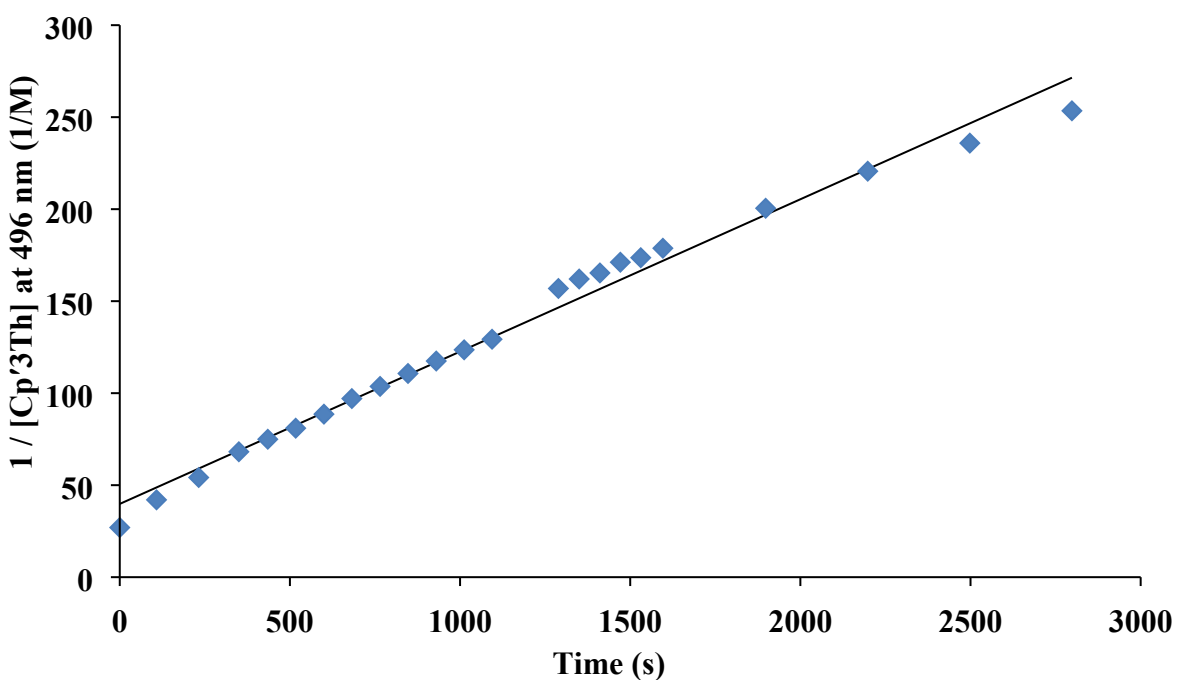


**Fig. S10.** Decomposition of A by monitoring absorbance at 496 nm in THF.

### **Electrochemical measurements of $\text{Cp}'_3\text{ThCl}$ .**

Data were collected using a glassy carbon working electrode, silver wire reference electrode, and platinum wire counter electrode. All data were collected in THF with 0.050 M  $[^7\text{Bu}_4]\text{[BPh}_4]$  as supporting electrolyte and ferrocene in solution as a standard. All scans were run in the negative direction to observe the cathodic wave.

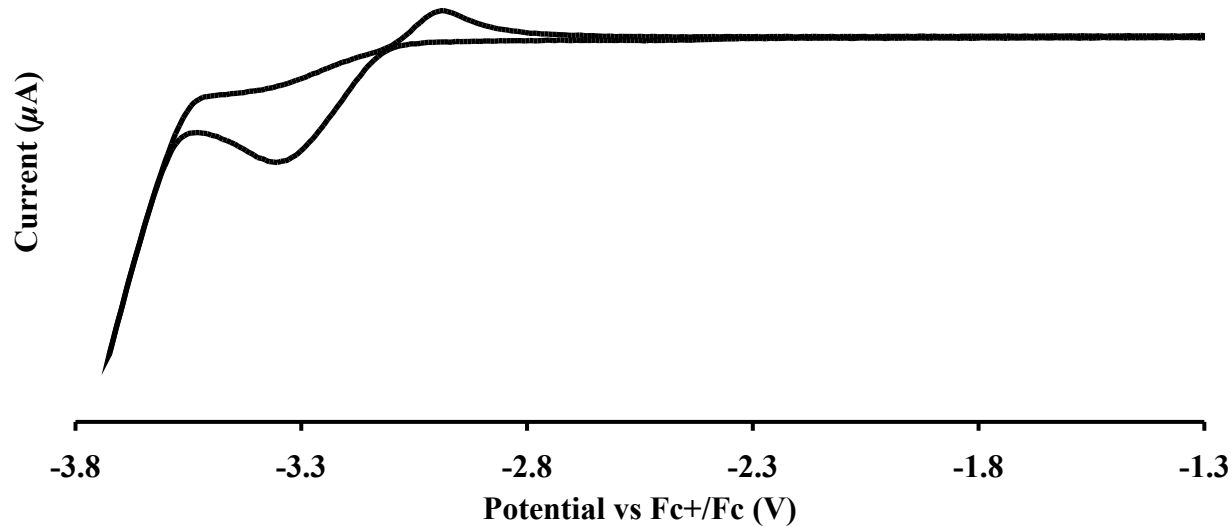


**Fig. S11.** Cyclic voltammogram of  $\text{Cp}'_3\text{ThCl}$  in 0.050 M  $[^7\text{Bu}_4]\text{[BPh}_4]$ /THF with a scan rate of 200 mV/s. Peak current ratio = 0.205, peak separation = 360 mV.

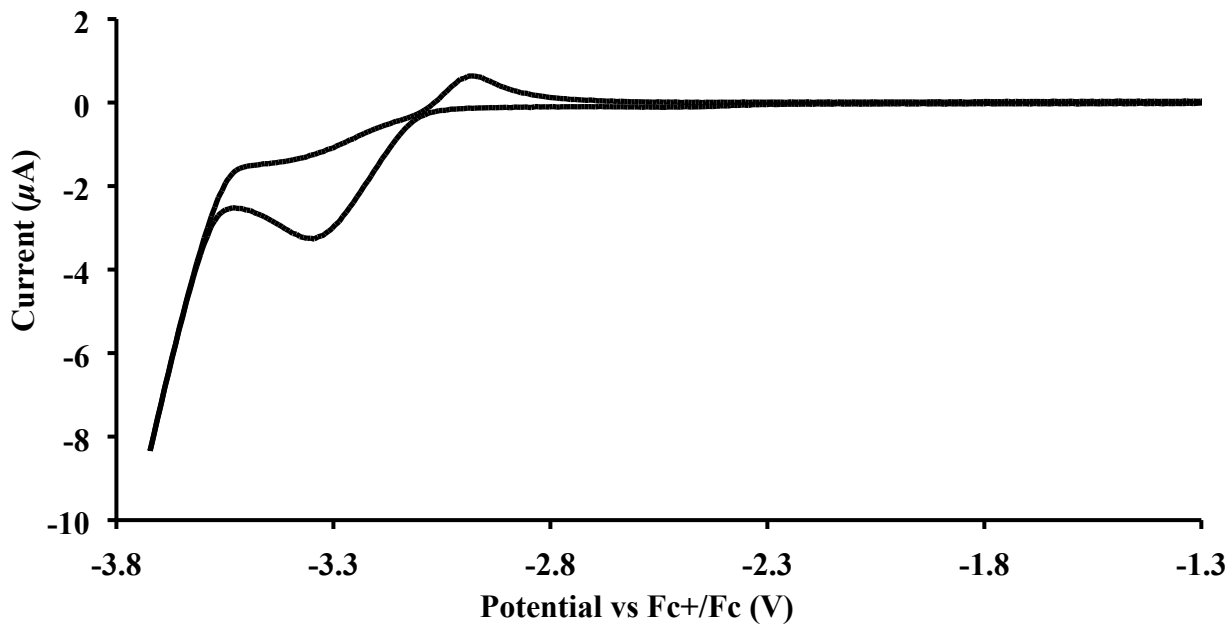


**Fig. S12.** Cyclic voltammogram of  $\text{Cp}'_3\text{ThCl}$  in 0.050 M [ ${}^\text{n}\text{Bu}_4\text{BPh}_4$ ]/THF with a scan rate of 500 mV/s. Peak current ratio = 0.195, peak separation = 380 mV.

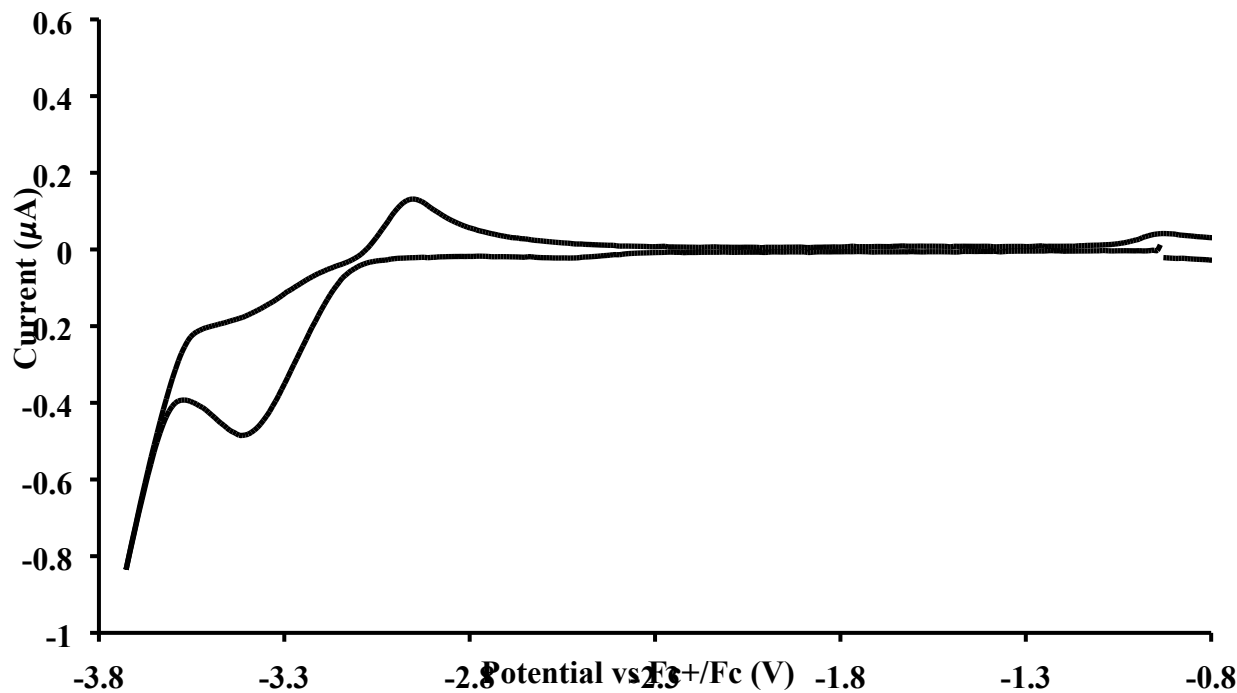


**Fig. S13.** Cyclic voltammogram of  $\text{Cp}'_3\text{ThCl}$  in 0.050 M [ ${}^\text{n}\text{Bu}_4\text{BPh}_4$ ]/THF with a scan rate of 1000 mV/s. Peak current ratio = 0.265, peak separation = 440 mV.

## **References**

1. M. Weydert, J. G. Brennan, R. A. Andersen, and R. G. Bergman. *Organometallics* 1995, **14**, 3942–3951.
2. APEX2 Version 2014.11-0, Bruker AXS, Inc.; Madison, WI 2014.
3. SAINT Version 8.34a, Bruker AXS, Inc.; Madison, WI 2013.
4. Sheldrick, G. M. SADABS, Version 2014/5, Bruker AXS, Inc.; Madison, WI 2014.
5. Sheldrick, G. M. SHELXTL, Version 2014/7, Bruker AXS, Inc.; Madison, WI 2014
6. International Tables for Crystallography 1992, Vol. C., Dordrecht: Kluwer Academic Publishers.
7. (a) A. L. Spek. *Acta Cryst.* 2015, **C71**, 9-19. (b) A. L. Spek. *Acta. Cryst.* 2009, **D65**, 148-155.
8. V. N. Staroverov, G. E. Scuseria, J. Tao, and J. P. Perdew. *J. Chem. Phys.* 2003, **119**, 12129–12137.
9. (a) S. Grimme. *J. Comput. Chem.* 2006, **27**, 1787-1799. (b) S. Grimme, J. Antony, S. Ehrlich, and H. Krieg. *J. Chem. Phys.* 2010, **132**, 154104.
10. W. Küchle, M. Dolg, H. Stoll, and H. Preuss. *J. Chem. Phys.* 1994, **100**, 7535.
11. X. Cao and M. Dolg. *J. Mol. Struct. (Theochem)* 2004, **673**, 203.
12. A. Schäfer, H. Horn, and R. Ahlrichs. *J. Chem. Phys.* 1992, **97**, 2571.
13. A. Klamt and G. J. Schüürmann. *Chem. Soc., Perkin Trans.* 1993, **2**, 799-805.
14. TURBOMOLE V7.2 2017, a development of University of Karlsruhe and Forschungszentrum Karlsruhe GmbH, 1989-2007, TURBOMOLE GmbH, since 2007; available from <http://www.turbomole.com>.

15. R. R. Langeslay, M. E. Fieser, J. W. Ziller, F. Furche, and W. J. Evans. *Chem. Sci.* 2015, **6**, 517–521.
16. R. Send, M. Kühn, and F. Furche. *J. Chem. Theory Comput.*, 2011, **7**, 2376–2386.
17. VMD 1.9, available from <http://www.ks.uiuc.edu/Research/vmd/>.
18. N. A. Siladke, C. L. Webster, J. R. Walensky, M. K. Takase, J. W. Ziller, D. J. Grant, L. Gagliardi, and W. J. Evans. *Organometallics* 2013, **32**, 6522–6531.
19. T. F. Jenkins, D. H. Woen, L. N. Mohanam, J. W. Ziller, F. Furche, and W. J. Evans. *Organometallics* 2018, **37**, 3863–3873.